Semiconductor Detectors

Francesco Forti, INFN and University, Pisa
Belle II Physics Week
29 November 2021

Università di Pisa
Dipartimento di Fisica
"Enrico Fermi"

Outline

- Introduction
- Semiconductor basics
- Junctions as sensors
- Strip detectors
- Pixel detectors
- Belle II PXD and SVD

Introduction

- Semiconductor detectors have been used for energy measurements since the 1960s
- In 1980s, the availability of microfabrication technology, with the possibility of structuring the electrodes at the 50-100μm level has vastly improved the position resolution, down to 10μm or even less.
- It has radically changed the way experiments are thought of and conducted
    - Secondary vertices from short-lived particles (like τ, B, D) become accessible
- Today, virtually every high energy physics experiment employs semiconductor detector
    - Unless the amount of material is unacceptable

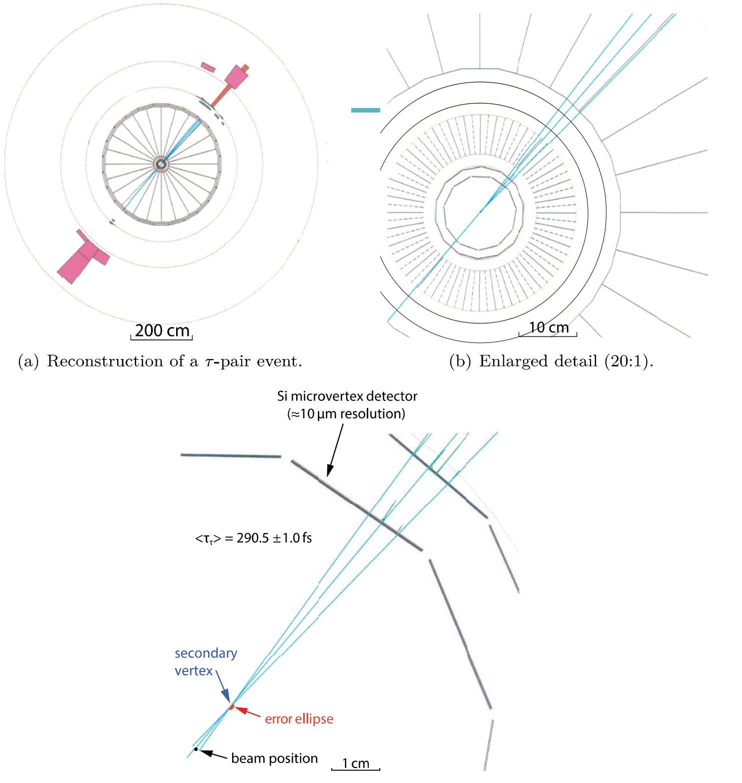

(a) Reconstruction of a τ-pair event. (b) Enlarged detail (20:1). (c) Enlarged detail (200:1).

Fig. 8.1 Event display of the reaction $e^+e^- \to Z^0 \to \tau^+\tau^-$ in which one of the two τ leptons decays into three pions. Panels (b) and (c) show enlarged details demonstrating the precise measurement of track hits in the silicon microvertex detector and the recognition of a so-called 'secondary vertex' (OPAL detector at the e^+e^- collider LEP, source: CERN).

$$e^+e^- \to Z^0 \to \tau^+\tau^-.$$

Starting point: gas ionization detectors

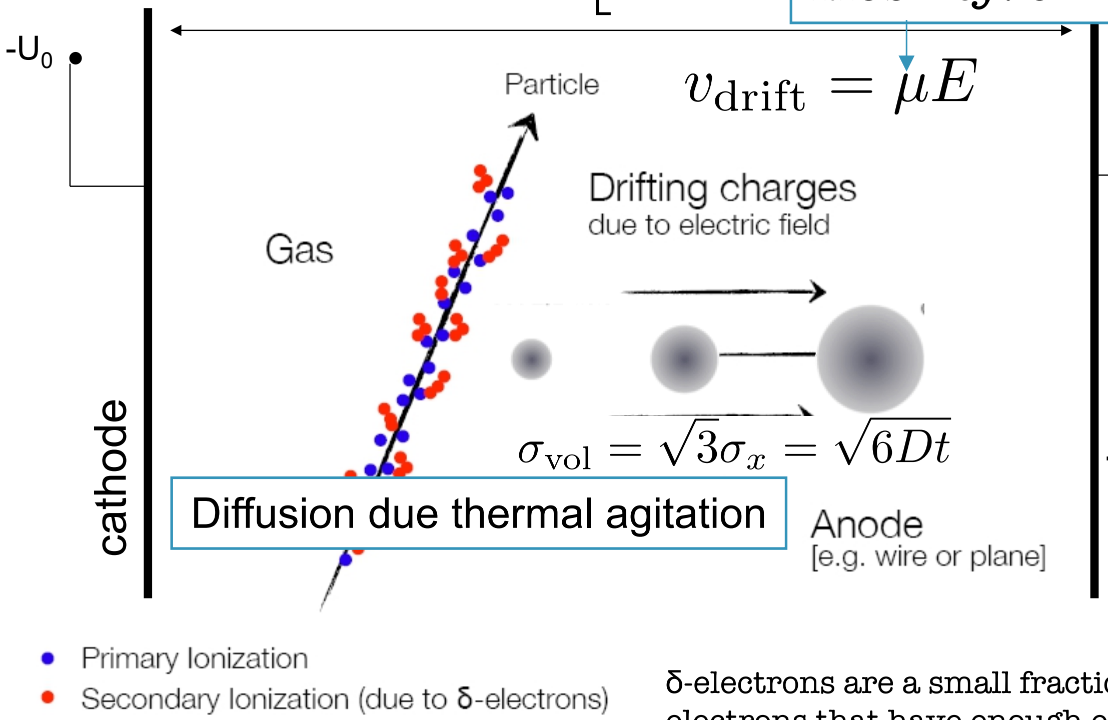

Mobility: drift in electric field

$$v_{\rm drift} = \mu E$$

Electrons: $v_d \sim cm/\mu s$

Ions: $v_d \sim cm/ms$

Diffusion due thermal agitation

$$\sigma_{\rm vol} = \sqrt{3}\sigma_x = \sqrt{6Dt}$$

D=Diffusion coefficient

$$D = \mu \frac{kT}{e}$$

δ-electrons are a small fraction of the ionization electrons that have enough energy to ionize other atoms

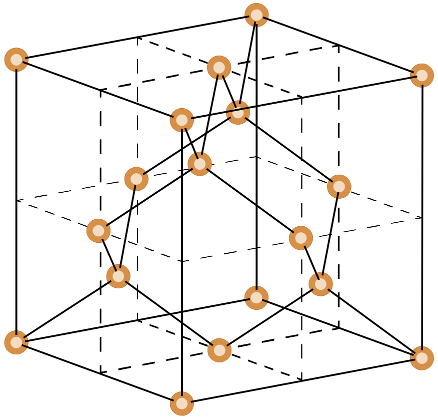

(a) Diamond lattice (Si, Ge).

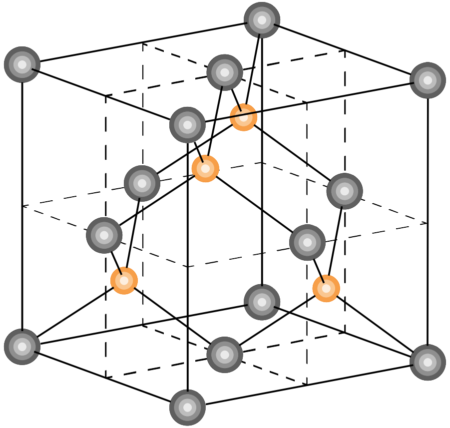

(b) Zinc blende (GaAs, CdTe).

Semiconductor basics

Refresher of semiconductor electronics

Table 8.1 Element and compound semiconductors.

Element	Compounds			
	IV–IV	III–V	II–VI	IV–VI
(C) Si Ge	SiC SiGe	AlP, AlAs, AlSb, BN, GaAs, GaP, GaSb, InAs, InP, InSb	CdS, CdSe, CdTe, ZnS, ZnSe, ZnTe, HgS, HgSe, HgTe	PdS, PbTe

Semiconductor ionization detectors

- Basic principle is the same as the ionization chamber
- But in semiconductors at non-zero temperature charge carriers are present, competing with ionization charge.

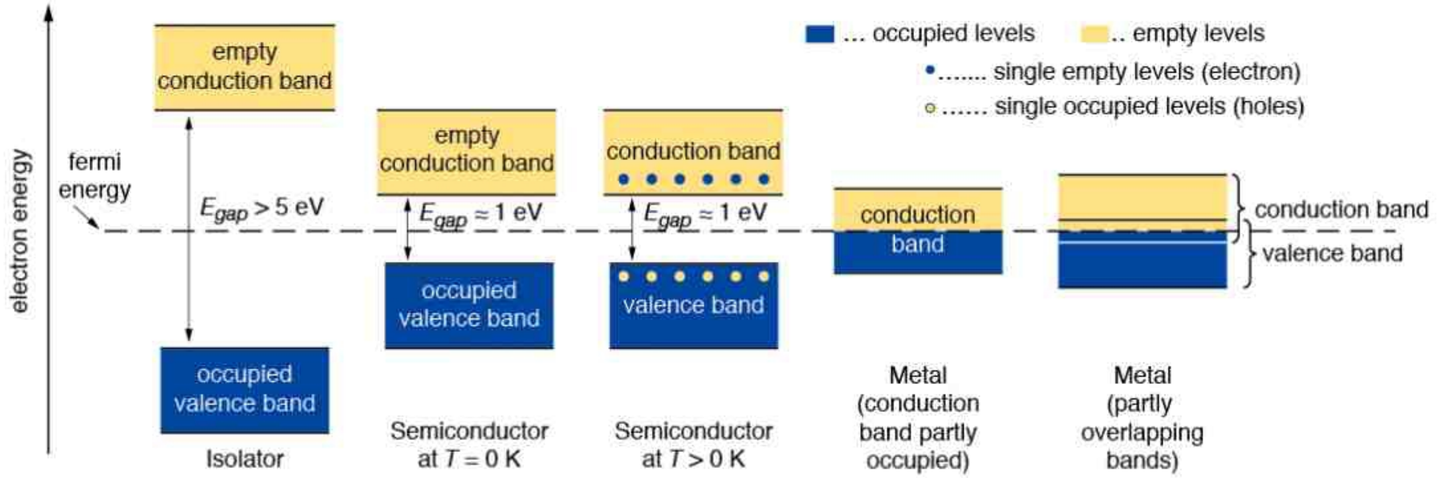

Intrinsic carrier concentration

- Because of the small band gap in semiconductors, at room temperature electrons can be excited to the conduction band, leaving holes in the valence band. And then recombine with holes.
- At thermal equilibrium a balance between excitation-recombination is reached leading to the "intrinsic carrier concentration"

$$n_e = n_h = n_i = 1.01 \bullet 10^{10} cm^{-3}$$

$$n_i = \sqrt{N_C N_V} \cdot \exp\left(-\frac{E_g}{2kT}\right) \propto T^{\frac{3}{2}} \cdot \exp\left(-\frac{E_g}{2kT}\right)$$

N_C, N_V =density of states at the edge of the conduction and valence band

- Because of this large intrinsic carrier concentration, if we polarize an intrinsic semiconductor a large current flows
- → cannot work as the ionization chamber

Intrinsic silicon

Band diagram | Density of states | Occupation probabilities | Carrier density

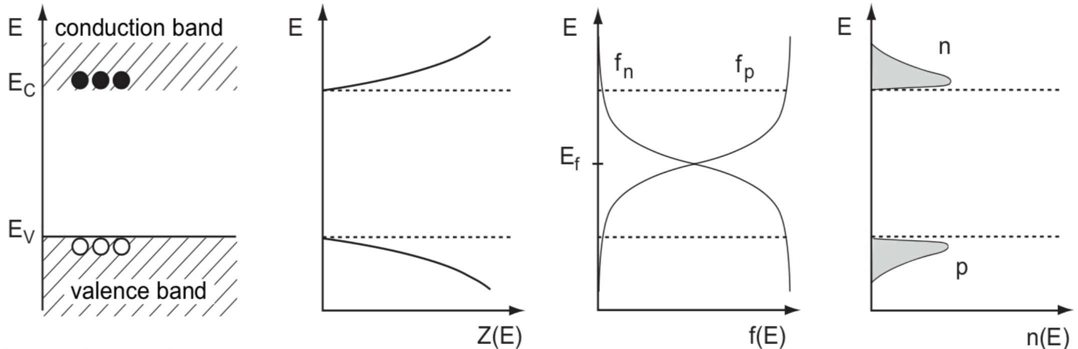

Kolanoski, Wermes 2015

(a) (b) (c) (d)

Carrier density

$$n_i \propto T^{3/2} \exp(-E_G/2kT),$$

$$\boxed{n_i \approx 1.01 \times 10^{10}\,\mathrm{cm}^{-3}\,.}$$

Conductivity and resistivity

$$\rho_i = [e(\mu_e + \mu_h)n_i]^{-1}$$

$$\rho_i \approx 320 k\Omega cm$$

[2] In the literature, for a long time $n_i = 1.45 \times 10^{10}\,\mathrm{cm}^{-3}$ was listed, a value which according to newer calculations [473, 904, 653] is no longer tenable, in agreement with measurements of the resistivity of intrinsic silicon [905].

Properties of intrinsic semiconductors

T=300K

Property	Si	Ge	GaAs	CdTe	Diamond
atomic number (Z)	14	32	31/33	48/52	6
atom mass (u)	28.09	72.60	72.32	120.0	12.01
density ρ (g/cm^3)	2.328	5.327	5.32	5.85	3.51
crystal structure	D	D	ZB	ZB	D
lattice constant (Å)	5.431	5.646	5.653	6.48	3.57
semiconductor type	indirect	indirect	direct	direct	indirect
band gap E_G (eV)	1.12	0.66	1.424	1.44	5.5
intr. carrier density (cm^{-3})	1.01×10^{10}	2.4×10^{13}	2.1×10^{6}	10^7	≈ 0
resistivity (Ω cm)	3.2x10^5	47	10^8	10^9	$\approx 10^{16}$
dielectric constant (ϵ)	11.9	16	13.1	10.2	5.7
radiation length X_0 (cm)	9.36	2.30	2.29	1.52	12.15
average energy for (e/h) creation (eV)	3.65	2.96	4.2	4.43	13.1
thermal conductivity ($\frac{W}{cmK}$)	1.48	0.6	0.55	0.06	>18
mobility ($\frac{cm^2}{Vs}$)					
electrons μ_n	1450	3900	8500	1050	≈1800
holes μ_h	500	1800	400	90	≈2300
lifetime					
electrons τ_e	>100 µs	~ms	1–10 ns	0.1–2 µs	≈100 ns
holes τ_h	>100 µs	~ms	20 ns	0.1–1 µs	≈50 ns

D=Diamond
ZB=Zinc blend

Doping: control density of carriers

N-type doping
P, As, Sb (5 e)

Donor: donates
an electron

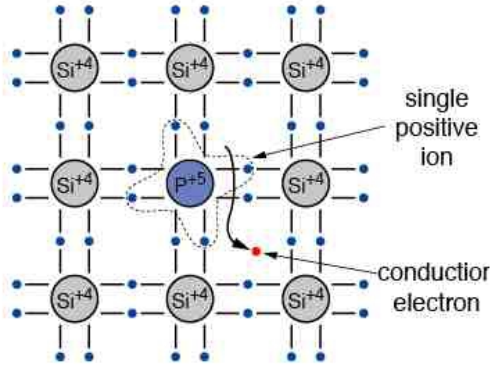

P-type doping
Al, B, Ga (3 e)

Acceptor: accepts
an electron

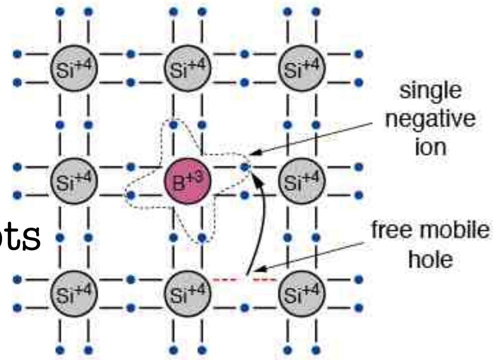

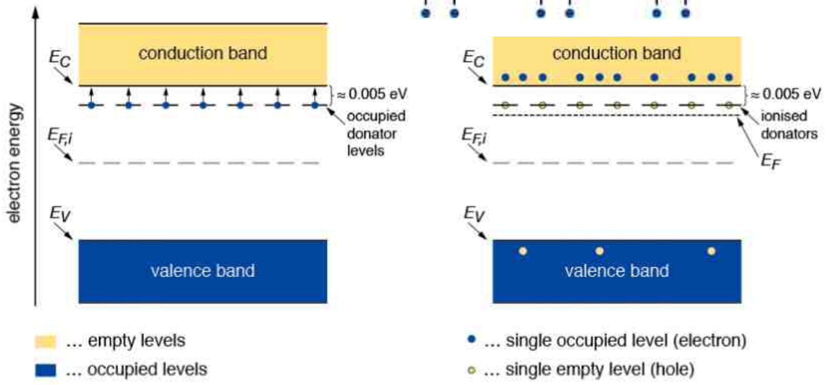

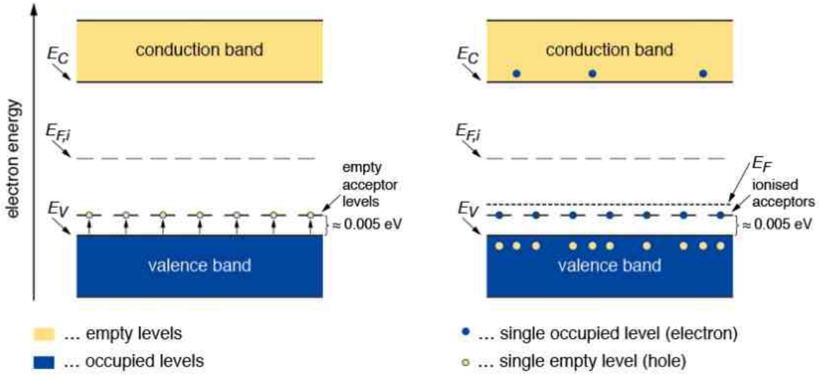

For N-type $n_e = N_D$

At equilibrium $n_e \bullet n_h = n_i^2$

For P-type $n_h = N_A$

N-Type example

- Electrons are the majority carriers:
  - density determined by the donor density

$$n \approx N_D \approx 10^{16}\,\mathrm{cm}^{-3},$$

- Holes are the minority carriers:
  - density determined by mass-action law

$$p \approx \frac{n_i^2}{N_D} \approx \frac{10^{20}}{10^{16}} = 10^4\,\mathrm{cm}^{-3}.$$

Fermi energy level shifted towards the conduction band

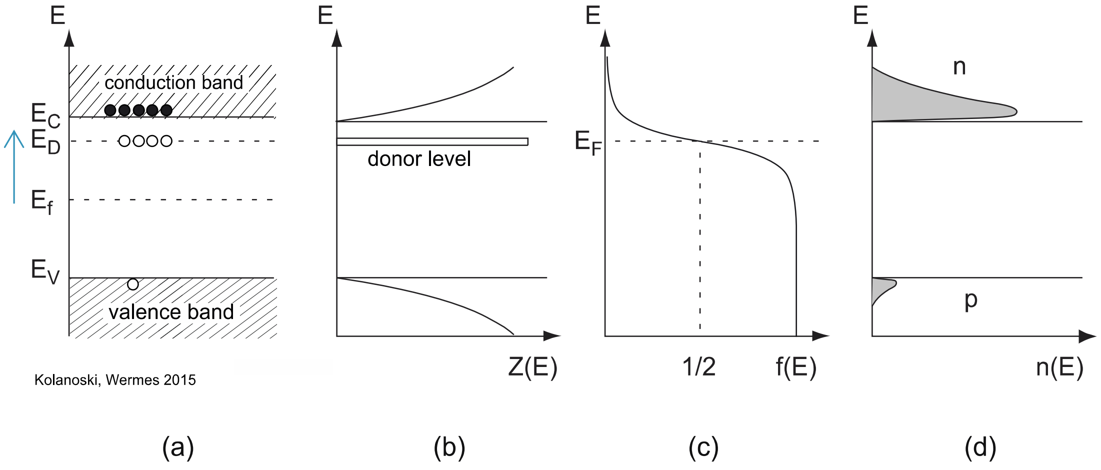

Junctions as sensors

How reverse-biased pn junctions can be used as sensors

Junction

- At the interface on n-type and p-type semiconductor the different electron/hole density causes diffusion.
  - Electrons from the n-type recombine with holes from the p-type
- An electric field is created by the fixed ions that remain behind (space charge)
  - At equilibrium the drift current from the electric field balances the diffusion current in the opposite direction
- The zone without free carriers (and with electric field) is called depletion zone

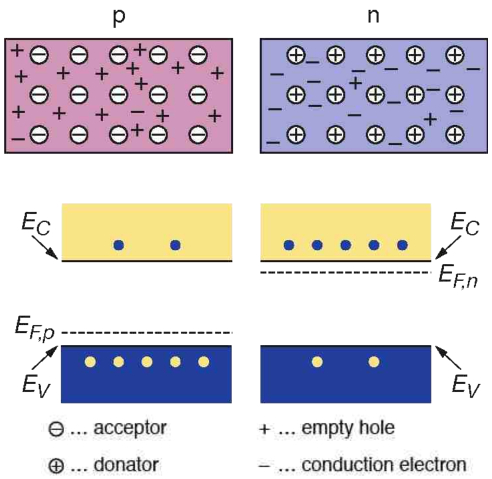

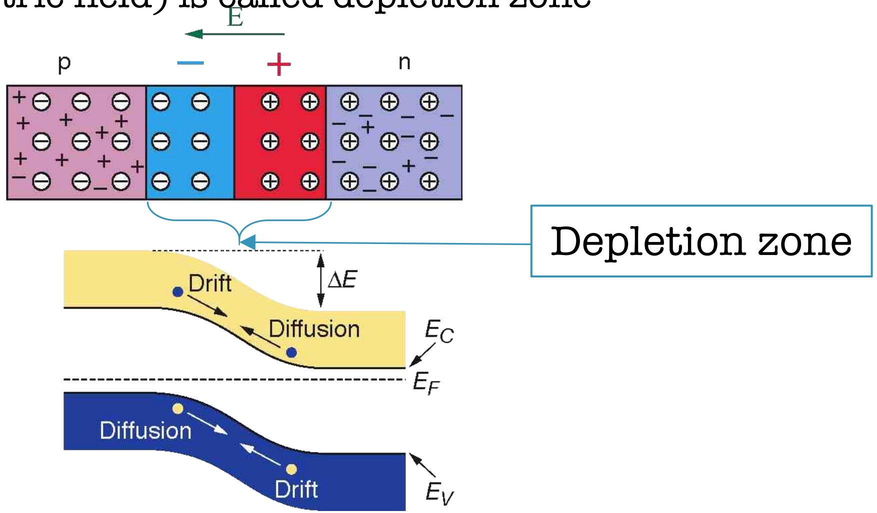

Depletion of sensor

The depletion is zone is the sensitive volume of the detector since generated ionization charge can be collected using the electric field

- Without external voltage the depletion zone is very small
- Applying an external reverse voltage one can extend the depletion zone
- The potential barrier between p and n is increased, and the current is very small (leakage current)

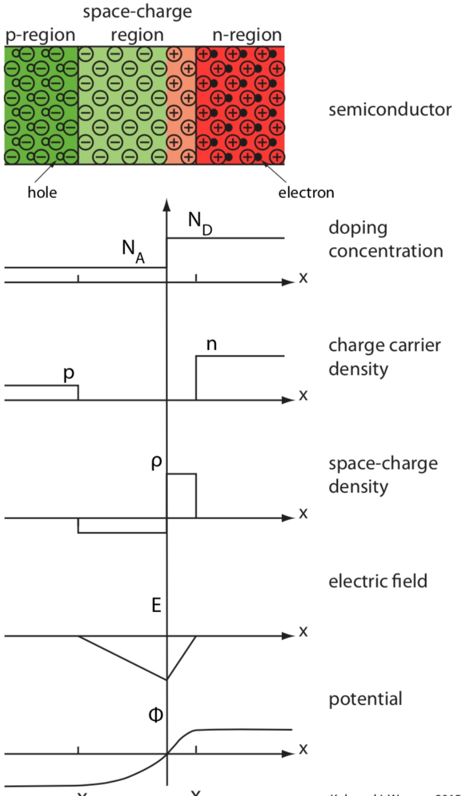

Kolanoski, Wermes 2015

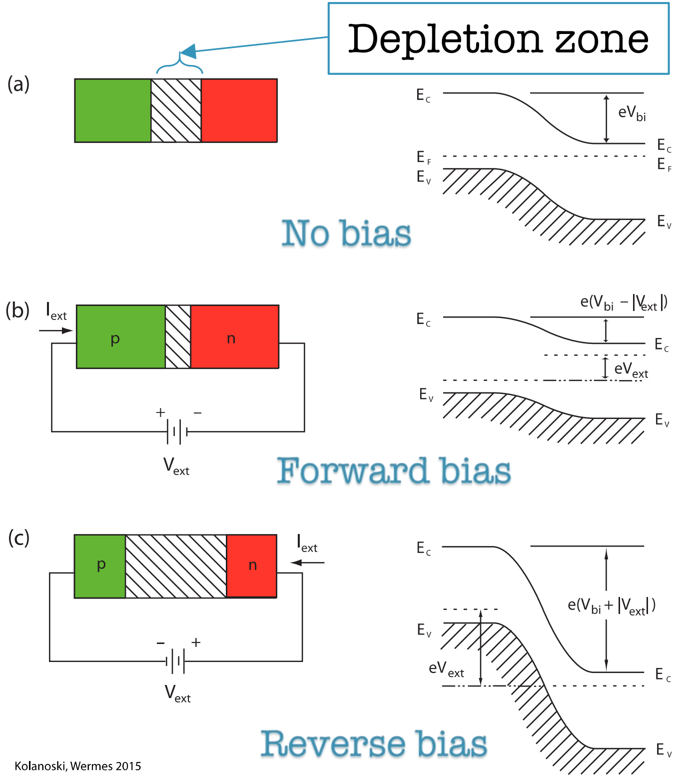

Kolanoski, Wermes 2015

Example of a typical p-n junction

Effective doping concentration $N_a = 10^{15}$ cm^{-3} in p+ region and $N_d = 10^{12}$ cm^{-3} in n bulk.

Without external voltage:

$$W_p = 0.02\ \mu m$$

$$W_n = 23\ \mu m$$

Applying a reverse bias voltage of 100 V:

$$W_p = 0.4\ \mu m$$

$$W_n = 363\ \mu m$$

$$d_n \approx 0.55 \sqrt{\frac{\rho}{\Omega\,\mathrm{cm}} \frac{V_{ext}}{\mathrm{V}}}\ \mu\mathrm{m}\,,$$

$$d_p \approx 0.32 \sqrt{\frac{\rho}{\Omega\,\mathrm{cm}} \frac{V_{ext}}{\mathrm{V}}}\ \mu\mathrm{m}\,,$$

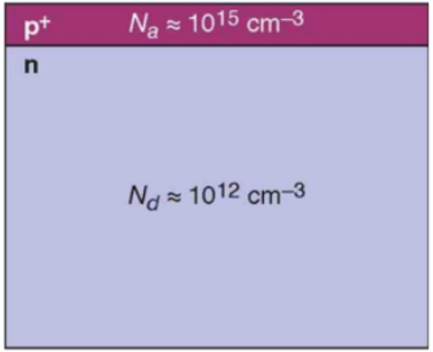

p+n junction

Width of depletion zone in n bulk:

$$\boxed{W \approx \sqrt{2\varepsilon_0 \varepsilon_r \mu \rho |V|}}$$

with $\rho = \dfrac{1}{e\,\mu N_{eff}}$

V … External voltage
ρ … specific resistivity
μ … mobility of majority charge carriers
N_{eff} … effective doping concentration

The depletion voltage is the voltage at which the depletion zone extends through the full thickness

Biasing the sensor

- To apply an external voltage to the sensor one needs metallic contacts and a bias resistor.
- The signal can in general be extracted from both sides
- A MIP in 320μm of silicon releases 24000 e- ~ 3.8fC (MPV): very small charge.
- Note: the detector bulk can be either p or n-type
- Need to make sure electric field does not cause breakdown

$$E = \frac{U}{d} = \frac{100\ \mathrm{V}}{300 \cdot 10^{-6}\ \mathrm{m}} \approx 3 \cdot 10^{5}\ \frac{\mathrm{V}}{\mathrm{m}}$$

[Safe. Breakdown limit at 10^7 V/m]

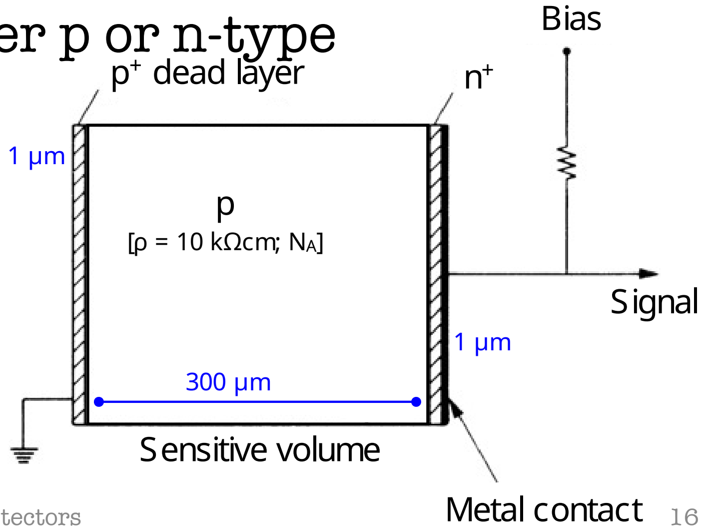

Sensor characterization

- Important parameters affecting noise are leakage current and sensor capacitance.
- Both depend on the depletion thickness $d \propto \sqrt{V}$ and saturate when full depletion is reached.

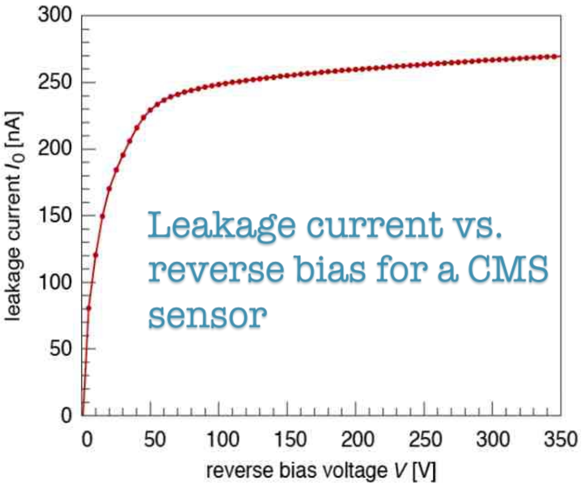

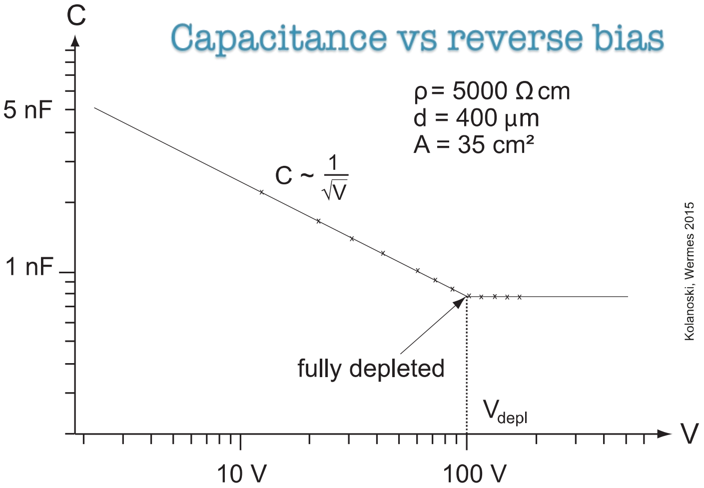

Note: for strip detectors, the interstrip capacitance dominates noise

Signal formation (ionization chamber)

- One electron-ion pair. Signal induced by **drift of charge** in the electric field. Shape depends on release point. Electrons much faster than ions.

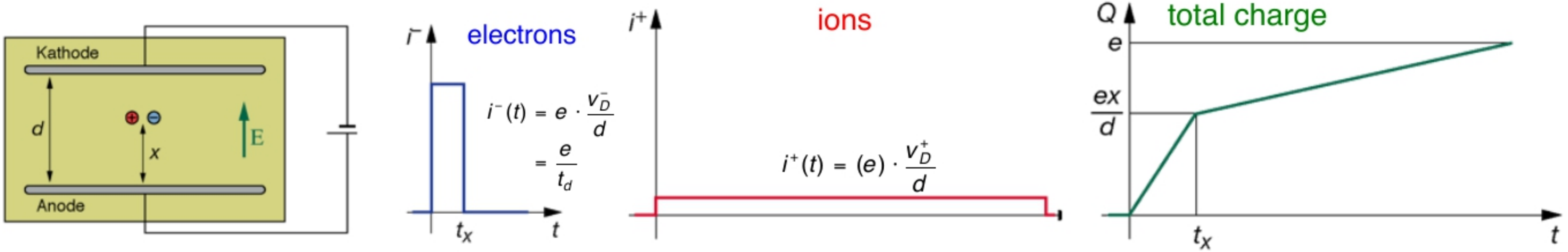

- Continuous charge generation when many charges released

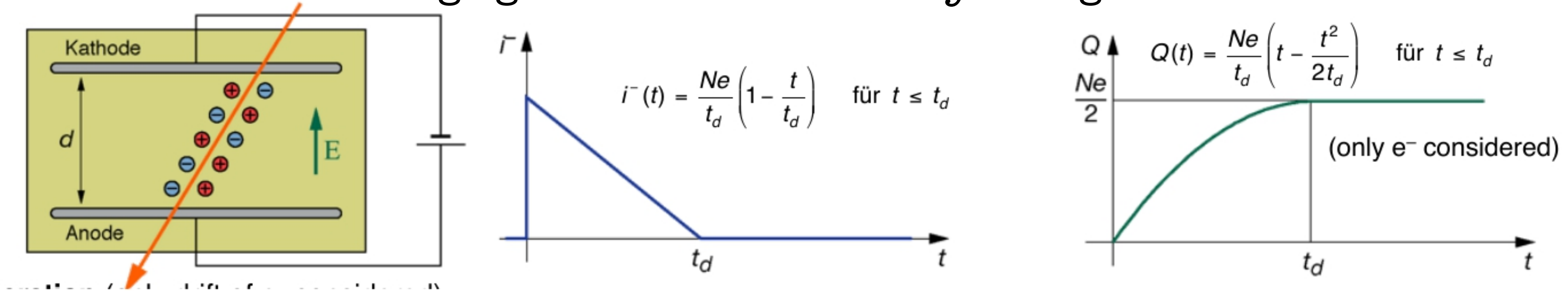

Charge collection in semiconductors

- Same concept:
  - signal generated as soon as the ionization charge starts to drift
- Electric field is not constant:
  - space charge implies linear E
  - more complicated behaviour
- Overdepletion:
  - bias with a voltage higher than the depletion voltage, resulting in faster signal collection
- Typical values for 320 um Silicon:
  - Collection time 5-10ns
  - Average charge: 34000 e/h pairs = 5 fC
  - Most probable ch: 24000 e/h pairs = 3.7 fC

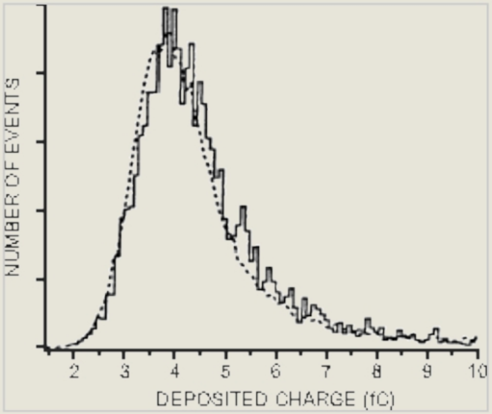

Fig. 1.17 Measured energy loss distribution of 1.5 MeV/c electrons in a silicon detector. The dashed line is a Vavilov theory calculation. (Wood *et al.* 1991. Figure courtesy of P. Skubic)

Semiconductor detector types

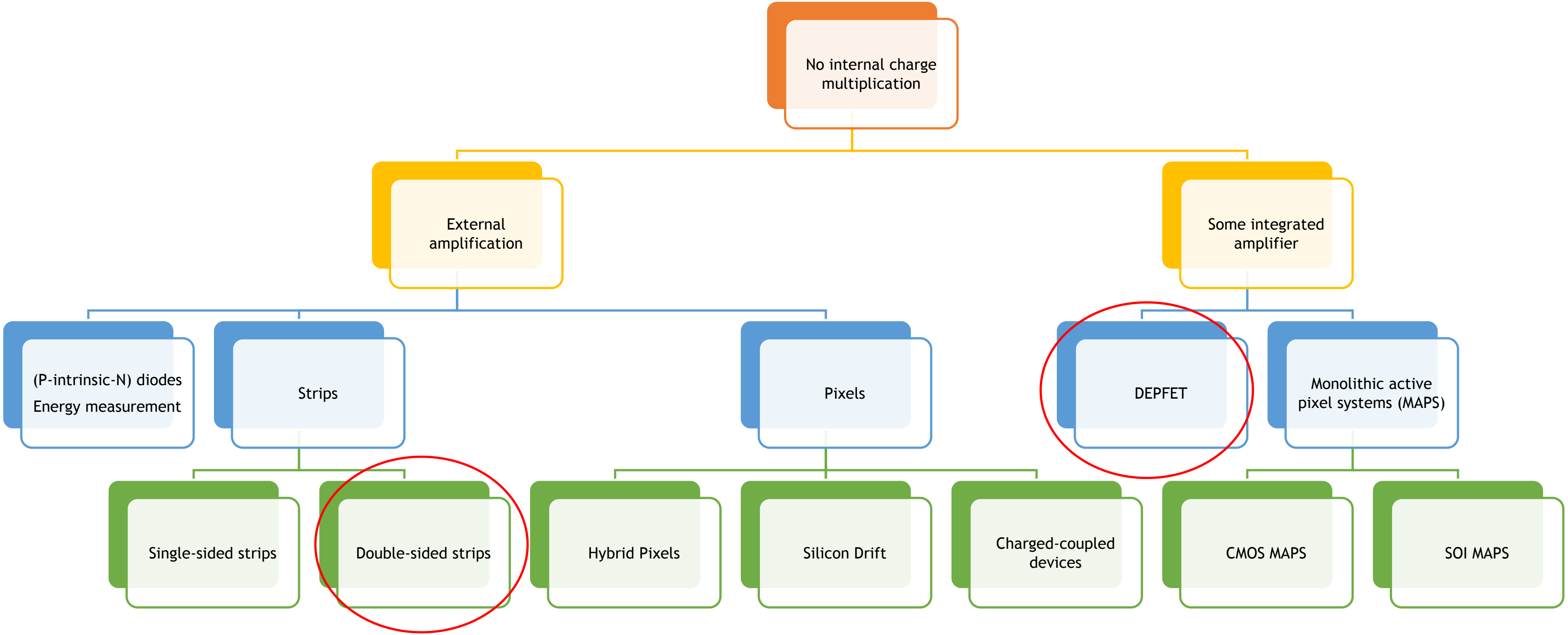

Strip detectors

Strip detectors

- Using modern microfabrication technology developed for electronics (planar process) one can segment the junction readout electrode in various ways → position sensitive detectors
  - Readout pitch can be as small as $50\mu m$
- Each electrode must have its own amplifier → need for miniaturized integrated circuits
- Signal to noise ratio requires careful optimization

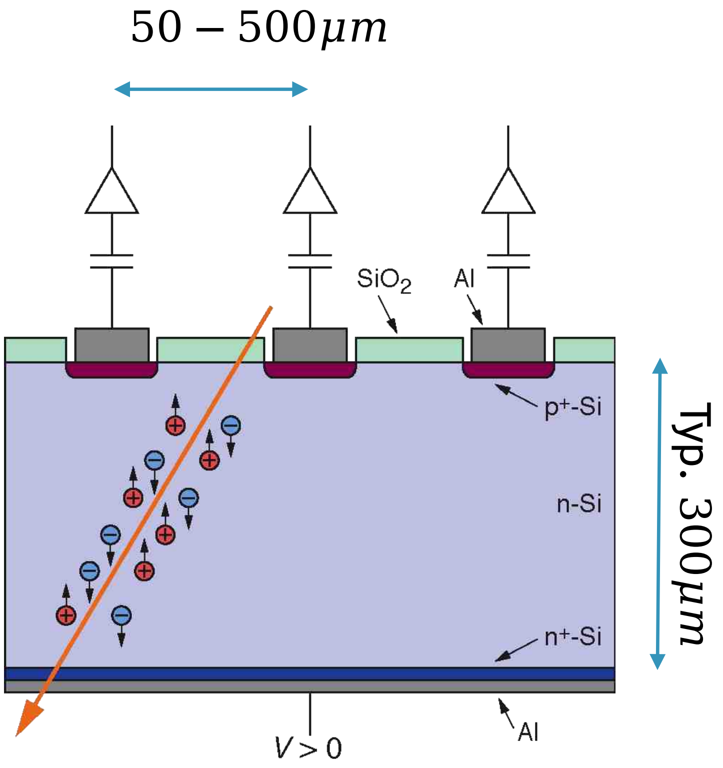

Coupling and bias

- It is desirable that leakage current does NOT flow into amplifier → AC coupling of strips
  - Integrate capacitors along the strip
  - SiO_2/Si_3N_4 deposition (100-200 nm)
  - Issues with defects of oxide (pinholes)
  - Order of 30pF/cm
- To apply voltage to the substrate a bias resistor is required
  - Can also be integrated on the detector surface
  - Deposition of polycrystalline silicon
  - Sheet resistance of order 250 $k\Omega/\square$ leading to a R~10 – 20 MΩ
  - Drawback: more fabrication complexity

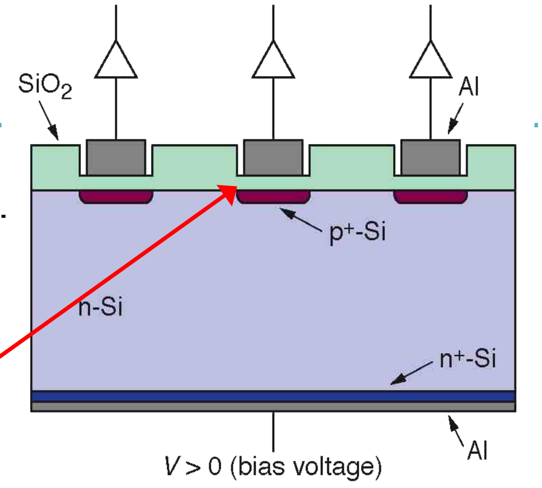

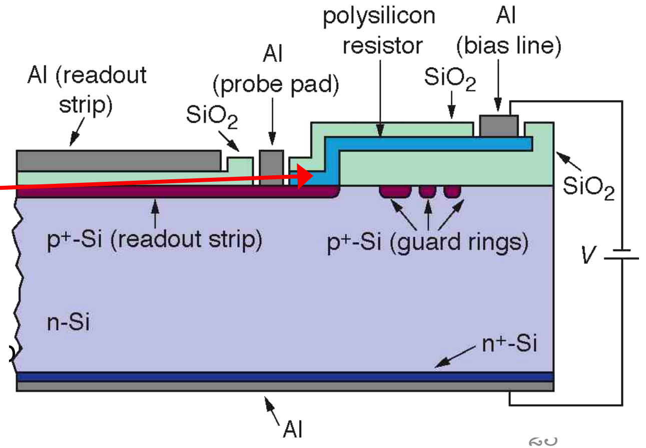

Point resolution

- Segmented detectors provide space information on the point x of passage of the particle
  - The distance between strips is called pitch p
- Point resolution depends on the readout mode and on the angle. For perpendicular tracks.
- Threshold readout (digital yes/no):
  - One strip is over threshold at position x_1.
  - Position estimator $x = x_1$
  - Flat probability between $x_1 - \frac{p}{2}$ and $x_1 + \frac{p}{2}$.
  - Resolution $\sigma_x = \frac{p}{\sqrt{12}}$
- Charge readout (analog)
  - Signals $h_1, \ h_2$ on strips at positions $x_1, \ x_2$
  - Position estimator center of gravity $x = \frac{x_1 h_1 + x_2 h_2}{h_1 + h_2}$
  - Resolution $\sigma_x \propto \frac{p}{\text{signal/noise}}$
  - Can take advantage of charge division through capacitive coupling

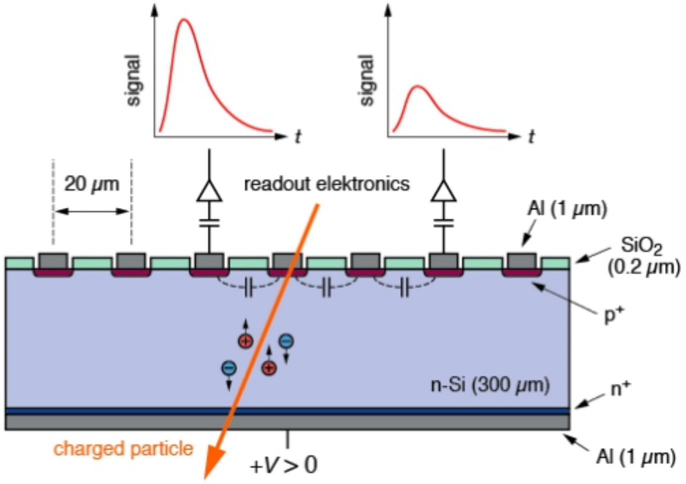

Inclined tracks

- Inclined tracks produce larger clusters: can improve resolution through interpolation (initially)
- At large angle the signal increases, but it is distributed on more strips
- If charge is subdivided among too many strips, noise dominates and resolution gets worse
- Smaller pitch is not always better.

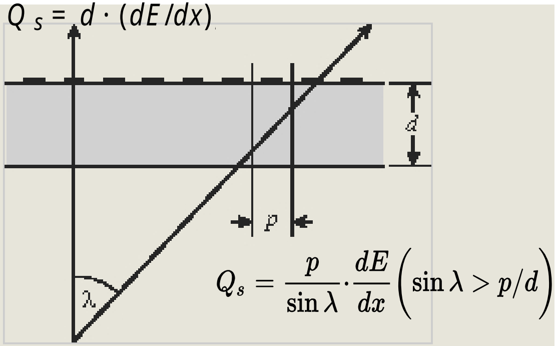

Fig. 8.4 As the dip angle λ increases the track traverses an increasing thickness of silicon. When the track subtends more than the strip pitch the signal is distributed over multiple strips, so the signal captured by one strip decreases.

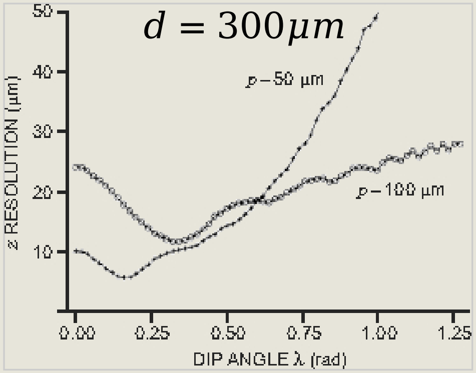

Fig. 8.3 z resolution for analog readout with interpolation *vs.* dip angle λ for strip pitches p = 50 and 100 μm and a signal-to-noise ratio of 20 at normal incidence (Lynch 1993).

1 floating strip

2-D detectors

- One needs to measure two coordinates of passage of a particle
- In principle can use two strips detectors with orthogonal orientation
  - Twice the material → bad impact on multiple scattering
- Development of double-side strip detectors
  - Need special insulating structures between n type strips (ohmic contact side)

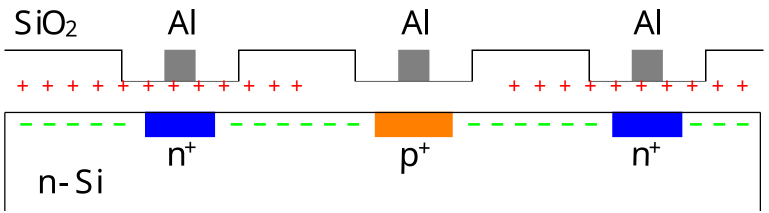

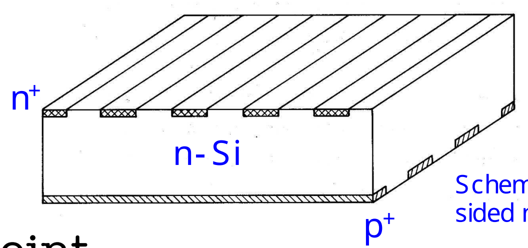

Schematics of a double sided micro-strip detector

- Same material as single sided, but 2D point
  - Ambiguity if more than particle crosses the detector: multiple combinations of the two views

Used in Belle II experiment

A personal gallery

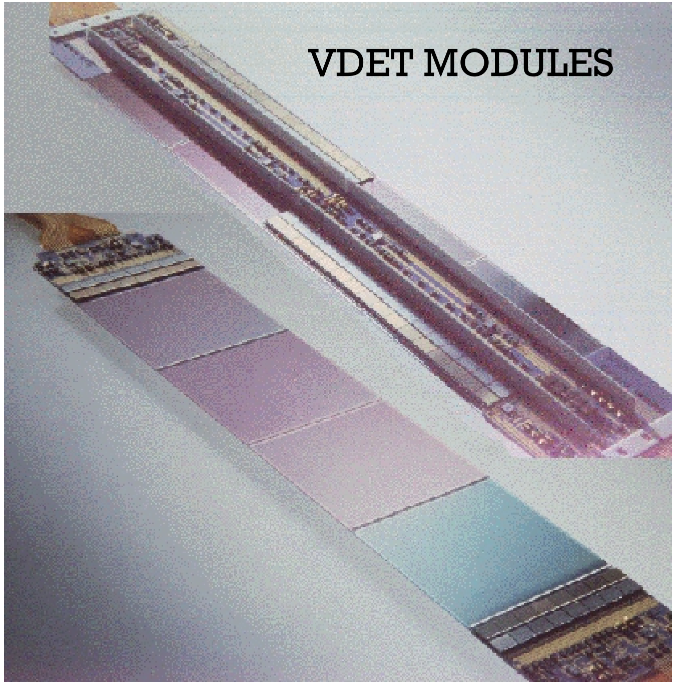

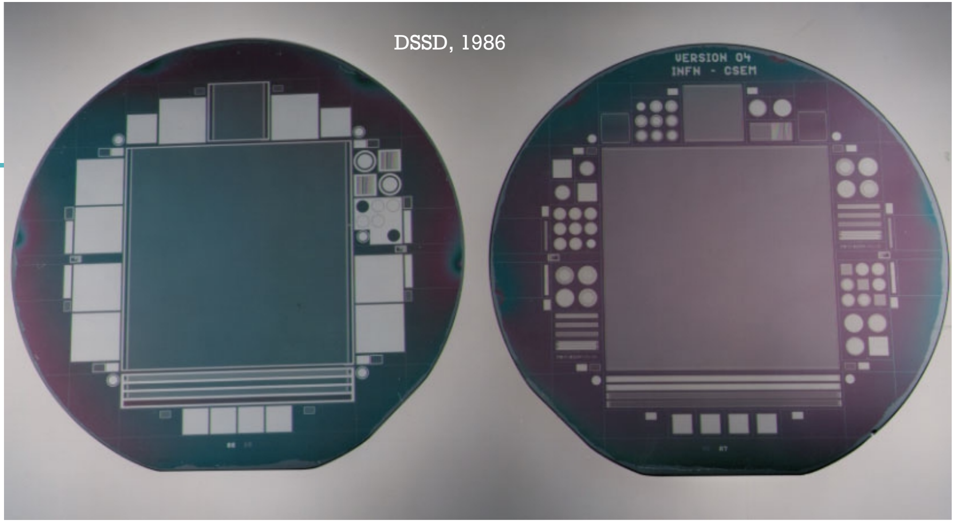

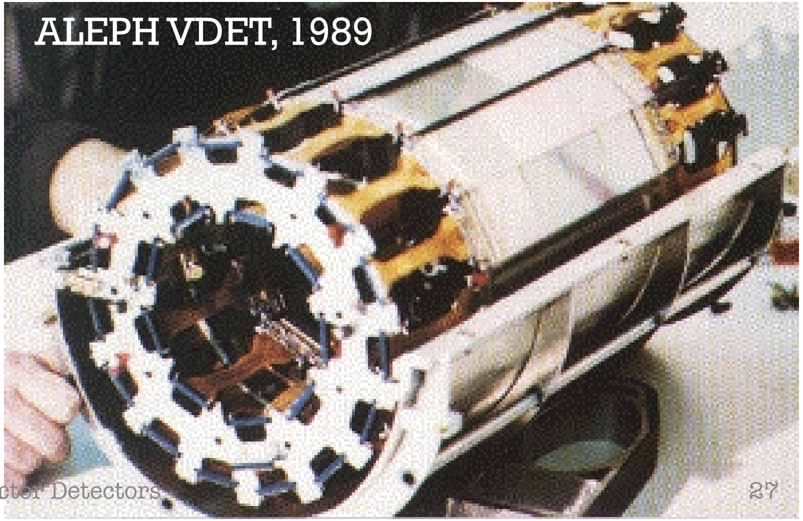

BABAR, 1999

- Lampshade

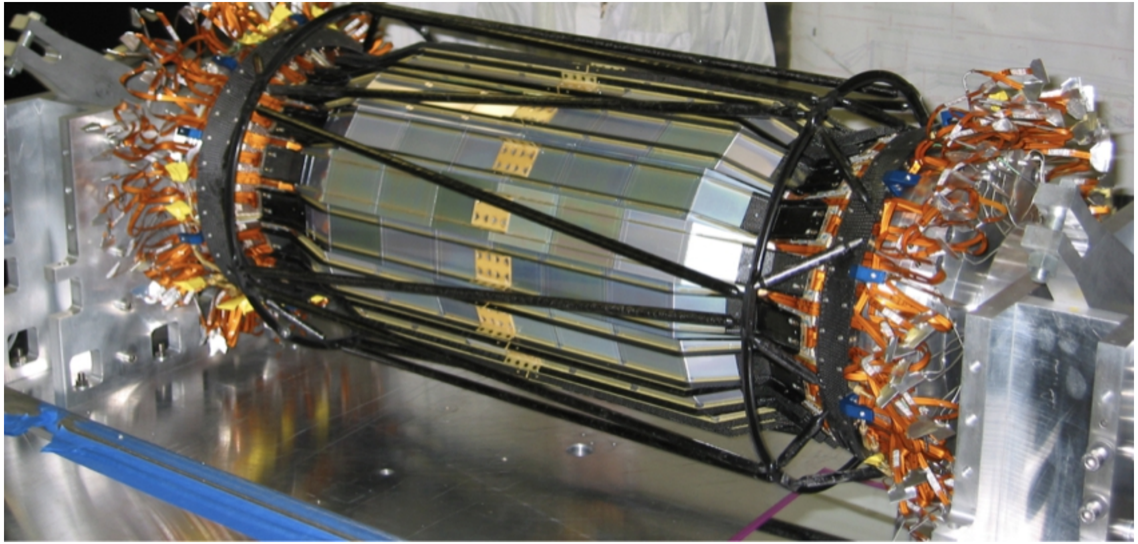

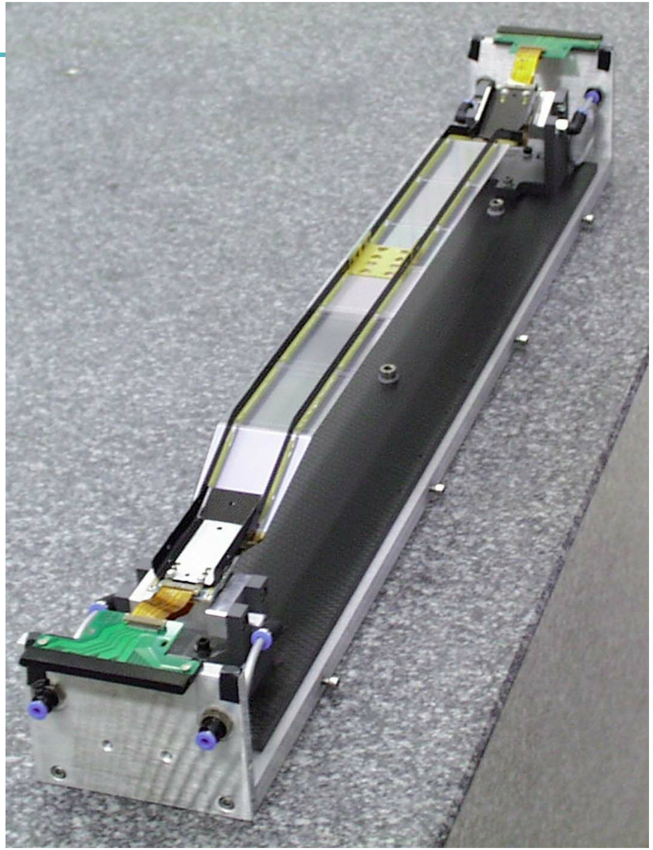

Belle II, 2019

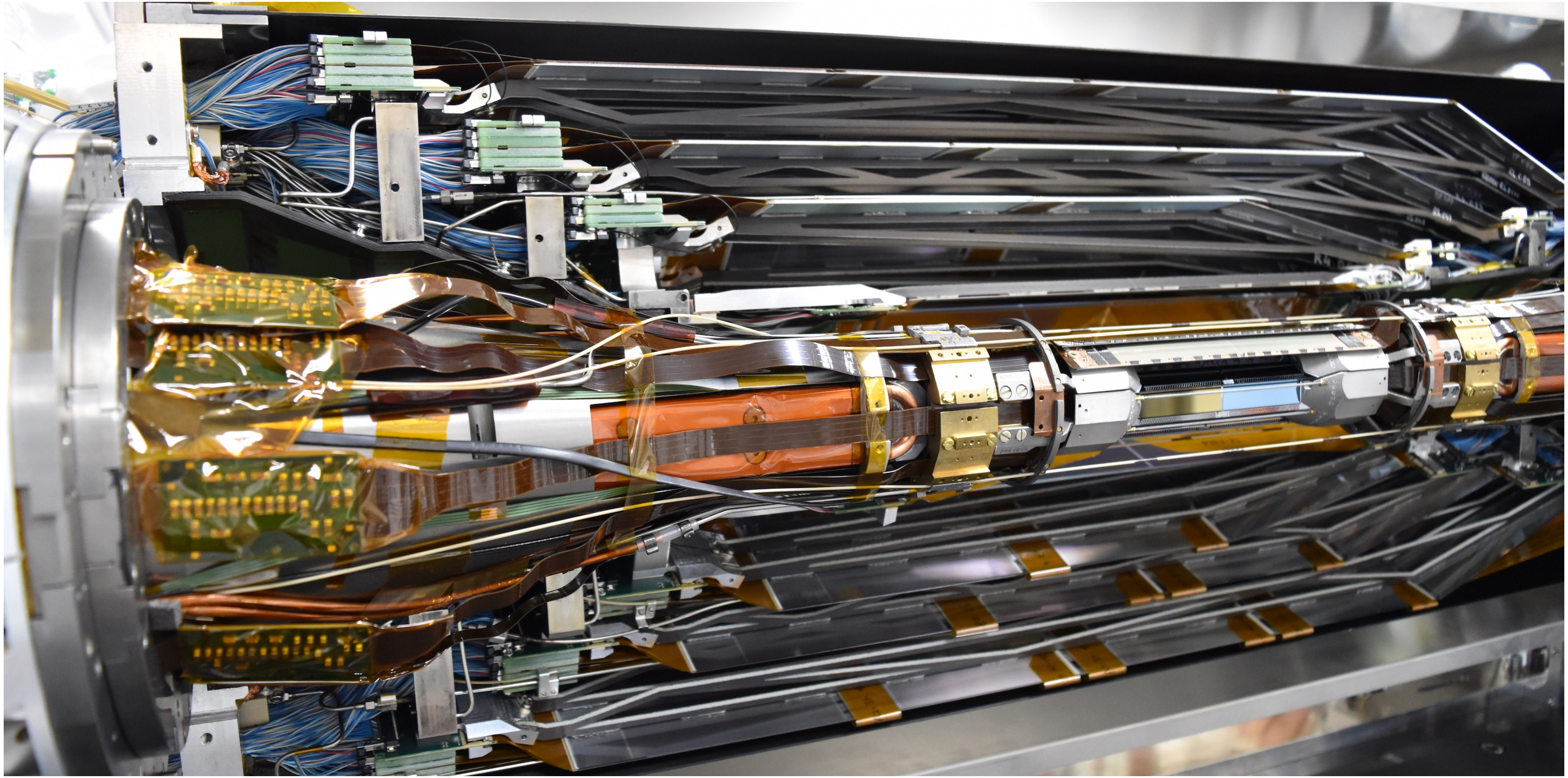

Pixel detectors

Hybrid and monolothic pixel detectors

Pixel detectors

- Electrodes can also be segmented in pixels
  - Pro: no ambiguity in point determination
  - Con: added complexity, huge number of channels
- Strong technology connection with digital cameras
- First development: Charged Coupled Devices (CCD)
  - Charged stored under metal gates, individually switchable. Slow readout
  - Pixel dimension down to $20\mu m$

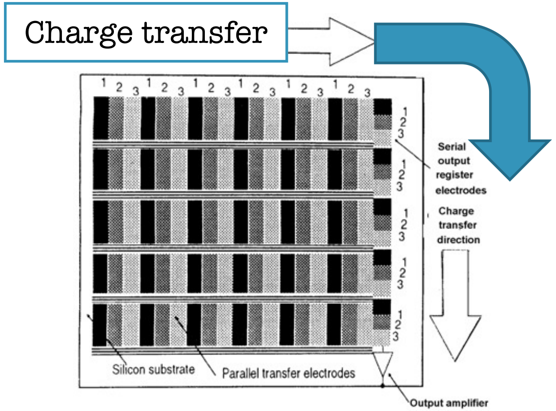

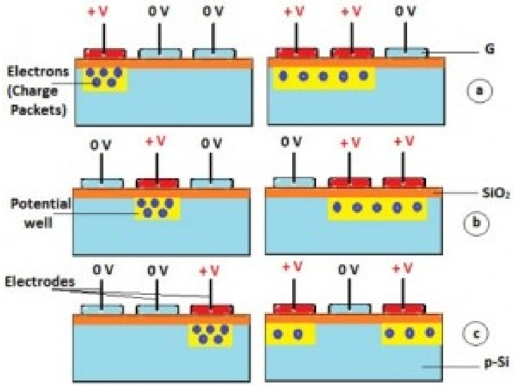

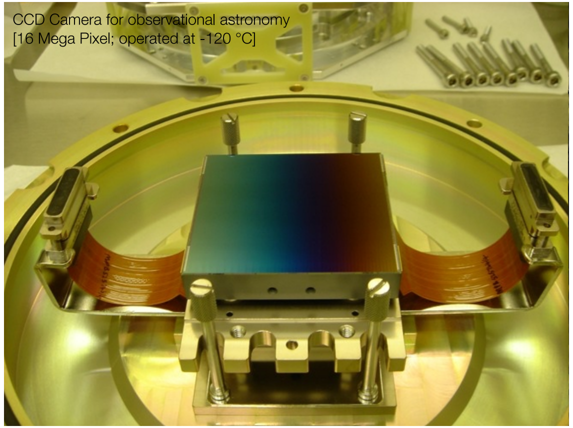

Flip-chip pixel detectors

- Sensor pixels are connected 1-to-1 to amplifier channels, organized with a matching geometry on the readout IC.
- Bump bonding technology: use soft material (like Indium) to perform vertical connection

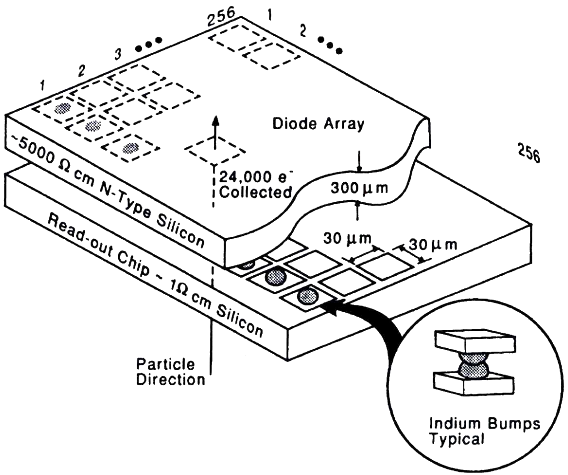

S.L. Shapiro et al., *Si PIN Diode Array Hybrids for Charged Particle Detection*, Nucl. Instr. Meth. A **275**, 580 (1989)

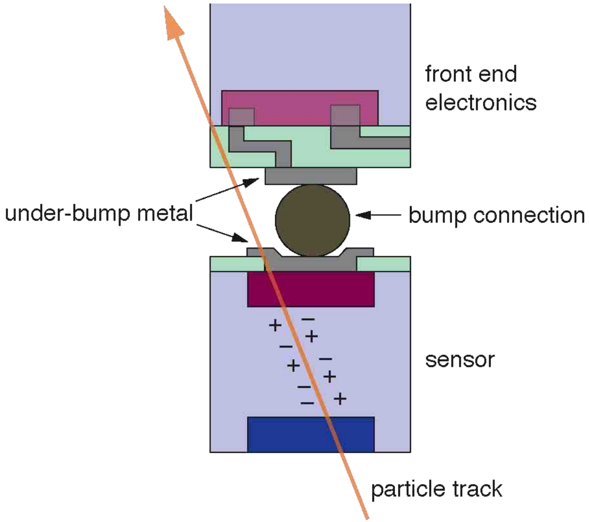

L. Rossi, *Pixel Detectors Hybridisation*, Nucl. Instr. Meth. A **501**, 239 (2003)

Motivation for monolothic detectors

- Hybrid pixels provide a very effective and performant system
  - Sensor and readout chip can be optimized separately.
  - Can be very fast and efficient
- But there are several issues:
  - Material of sensor + readout chip sum up
  - Interconnection technology not always reliable
  - Construction procedure is complex and expensive
- Both sensor and readout IC are silicon
  - Try to implement the two functions on the same substrate
  - But fabrication processes and details of the materials are quite different.
  - Sensor is high resistivity, electronics low resistivity
  - Sensor limits high temperature steps to keep current low, electronics typically has several high temperature steps
  - Developing special technologies very expensive and difficult
  - Motivation also with societal challenges

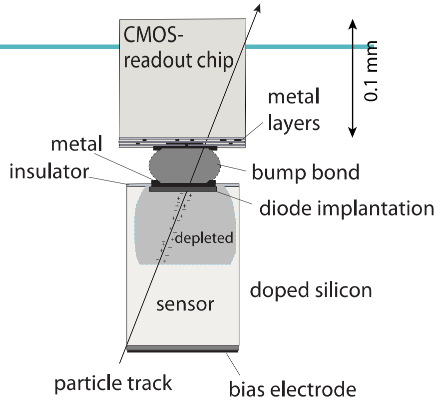

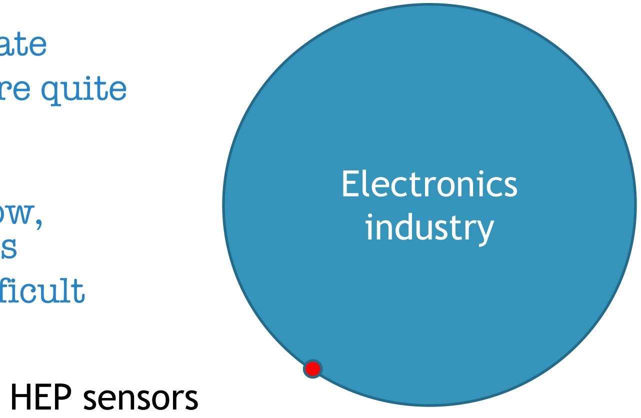

DEPFET

- Use the collected charge as a backgate for a FET transistor
- Provides internal electronic amplification
- Potential for extremely thin devices

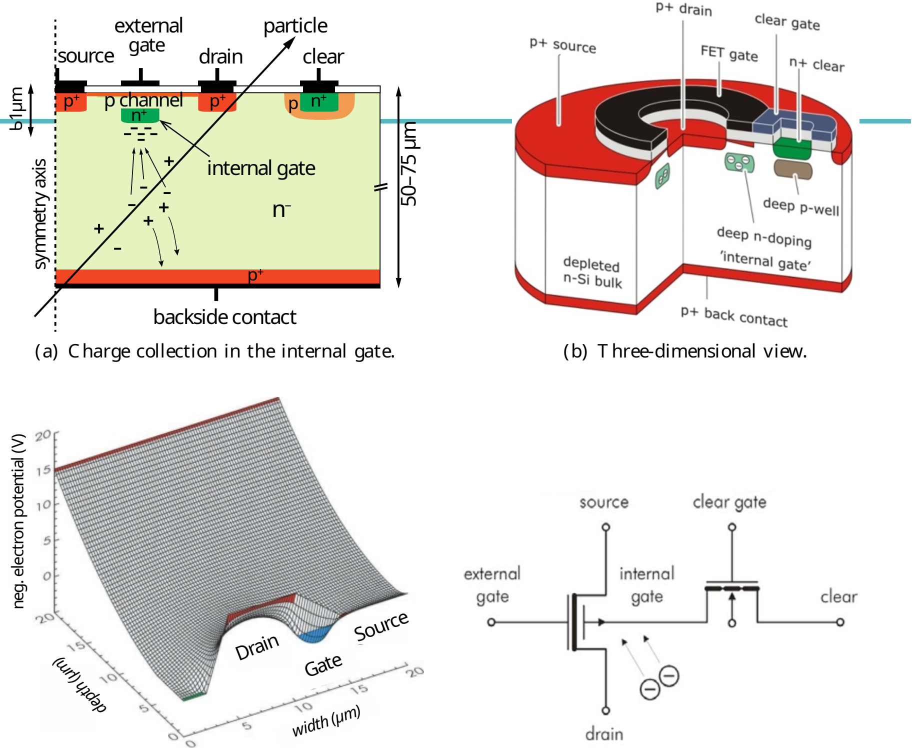

(a) Charge collection in the internal gate.

(b) Three-dimensional view.

(c) Electron potential.

(d) Electronic representation.

Fig. 8.67 DEPFET pixel: (a) cross section of one half of a circular DEPFET pixel cell with drawn symmetry axis; (b) three-dimensional view with visible additional elements needed for the operation like the *clear gate* [140]; (c) shape of the electrostatic potential for electrons near the transistor with a minimum (for electrons) at the internal gate (blue); maxima are indicated by the read areas; (d) electronic circuit representation.

DEPFETs

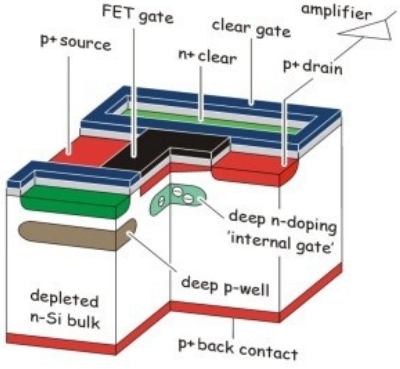

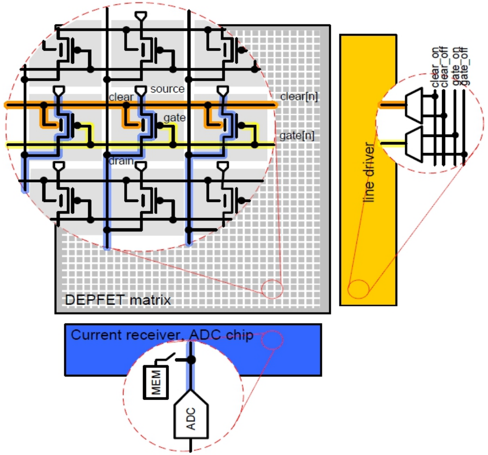

- **fully depleted sensitive volume**
  - fast signal rise time (~ns), small cluster size
- In-house fabrication at MPS Semiconductor Lab
  - **Wafer scale devices possible**
  - **Thinning to (almost) any desired thickness**
  - no stitching, 100% fill factor
- no charge transfer needed
  - faster read out
  - better radiation tolerance
- **Charge collection in "off" state, read out on demand**
  - potentially low power device
- **internal amplification**
  - charge-to-current conversion
  - r/o cap. independent of sensor thickness
  - **Good S/N for thin devices ~40nA/µm for mip**

Used in Belle II experiment

CMOS sensors

- Idea: use the CMOS Image Sensor (CIS) technology for particle detection. Electronics and sensor on the same substrate

Basic CIS technology

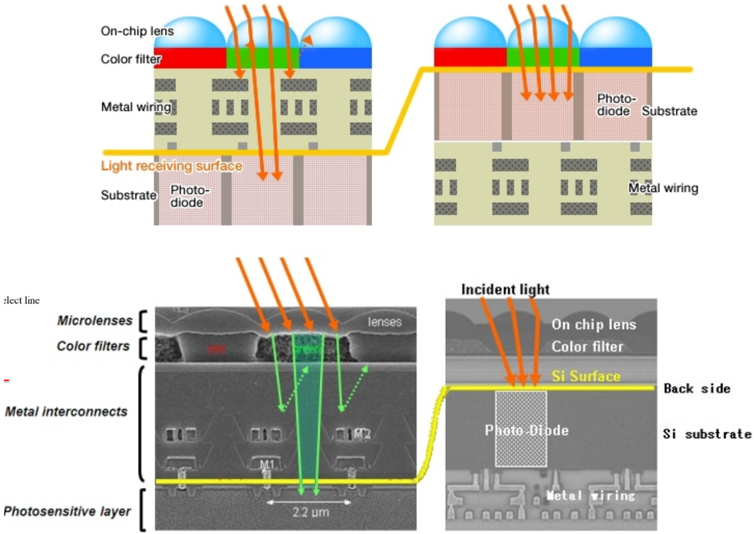

CMOS radiation sensor

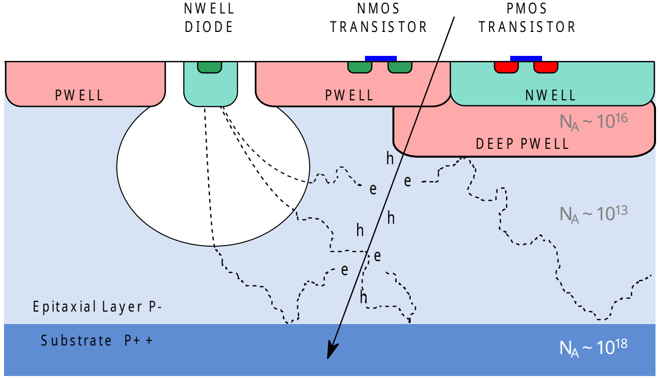

pixel capacitance C5 fF (@ V_{bb} = -3 V)

Very active development of many different structures

Belle II PXD and SVD

Belle II Vertex Detector

- VXD Requirements
  - Better resolution of tracks at the IP w.r.t Belle to compensate reduced boost: improved point resolution, reduced radius & low material
  - Operate in high background environment
    - Hit rates: 20-1.5 MHz/cm^2 @ R =14 - 40 mm
  - Radiation hard
    - 2–0.1 Mrad/yr @ R = 14 - 40 mm
- Pixel Detector (PXD)
  - DEPFET pixel sensors: Layer 1-2
  - Essential for vertex resolution
- Silicon Vertex Detector (SVD)
  - Double-sided Si strip sensors: Layer 3-4-5-6
  - Standalone tracking and PID of low p_T particles
  - Extrapolate tracks to PXD (Region of interest)

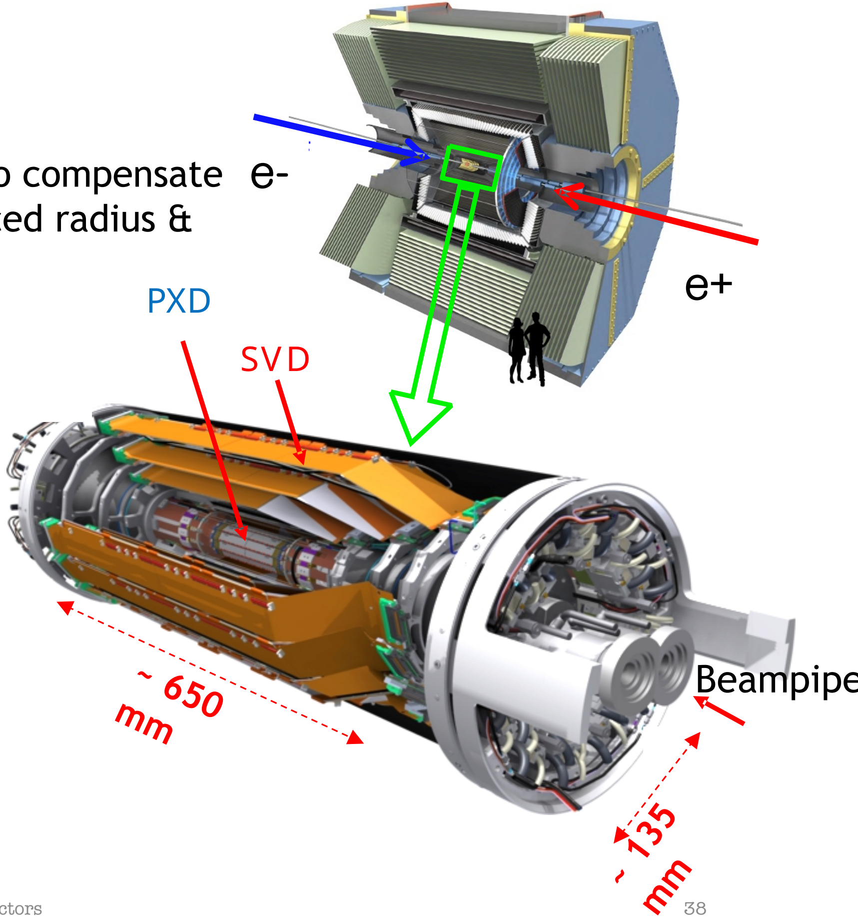

Silicon vertex detectors size comparison

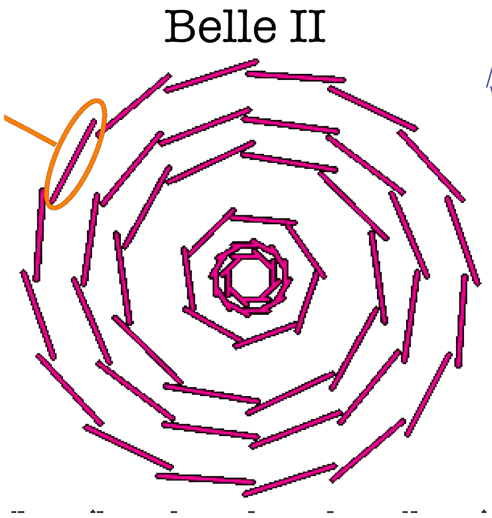

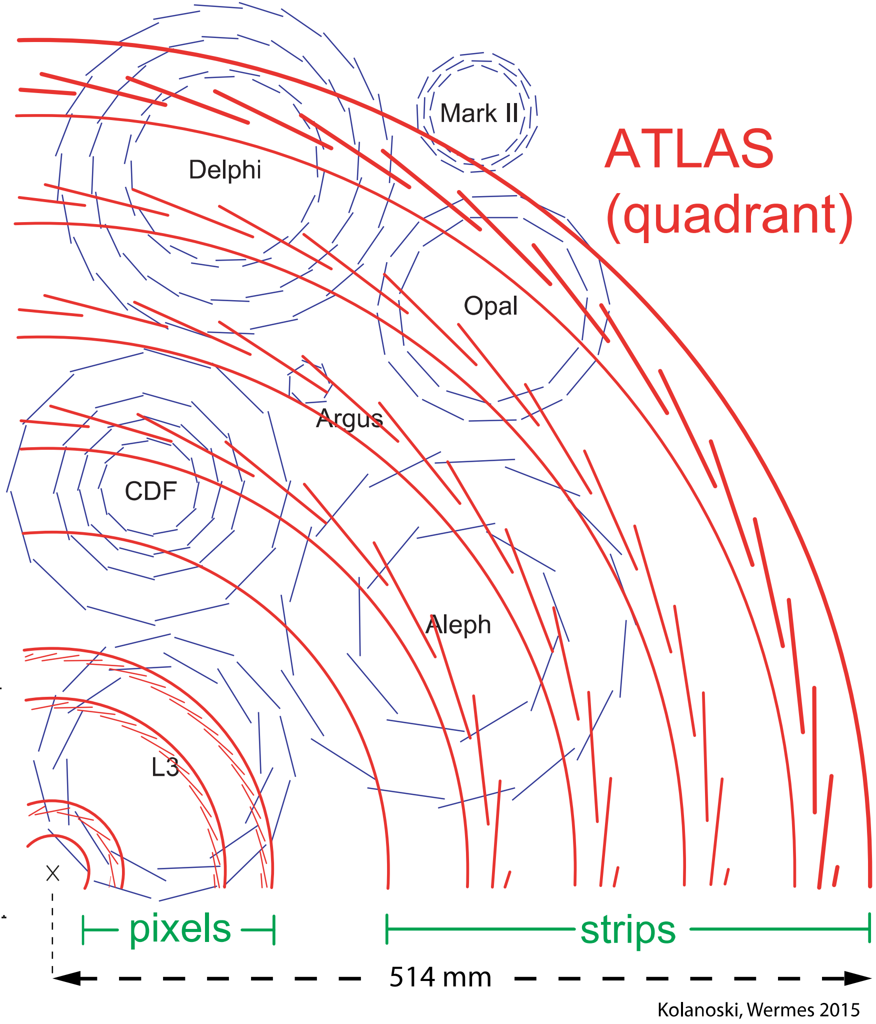

Fig. 8.52 Size comparison of various silicon detectors that have been installed in present and past collider experiments. The various smaller (vertex) detectors (all strip detectors) are compared with the size of one quarter of the ATLAS tracker (in red) consisting of pixels and strips. Not shown here is the semiconductor tracker of the CMS experiment [753, 297] consisting of silicon microstrip and pixel detectors with an outer radius of 1.25 m.

PXD

- Pixel Vertex Detector (PXD):
  - 2 layers of DEPFET sensors.
  - 8 inner ladders at radius 14 mm.
  - 12 outer ladders at radius 22 mm (only 2 ladders installed).
  - ~7.7 x 10^6 pixels.
  - ~0.21% X_0 / layer material budget.

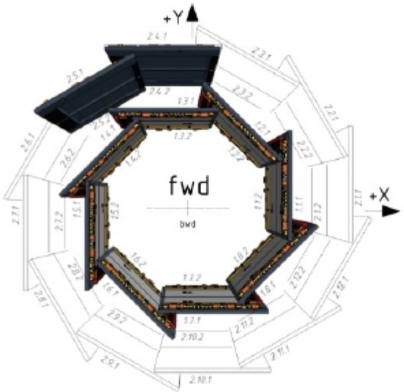

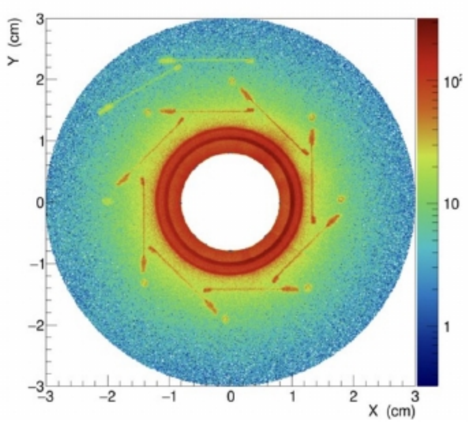

Scatter plot from data

DEPFET system

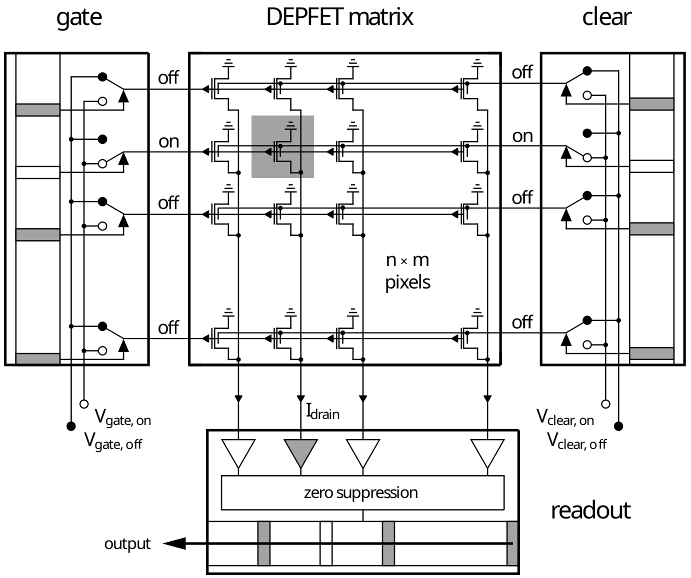

Fig. 8.69 Readout scheme of a DEPFET matrix. The gate chips address the rows one-by-one. The transistor drain lines (outputs) are routed to the readout chip(s) column-wise (bottom). Thereafter the charges in the internal gates of the row are cleared (clear).

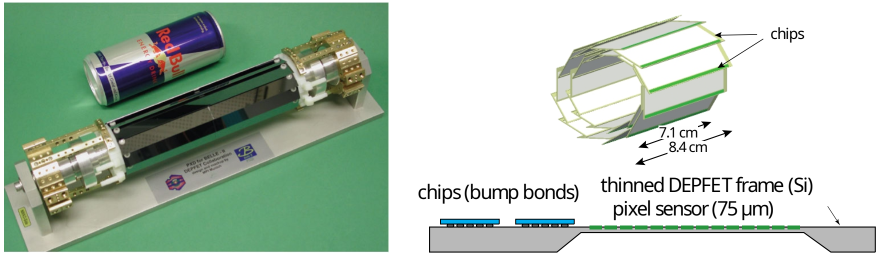

(a) Pixel vertex detector (PXD) of Belle II (model)

(b) Thinned DEPFET pixel module

Fig. 8.70 DEPFET pixel vertex detector PXD (Belle II). (a) Model (source: Belle II PXD Collaboration). (b) Cross section through a pixel module perpendicular to the beam. The active area of the sensor is thinned from the backside by an etching process [96] to 75 μm. The thick regions serve as support structures. On them the steering and readout chips are placed. The active area has dimensions $44.8 \times 12.5\,\text{mm}^2$. Module ladders contain two modules each. The radii of the DEPFET pixel layers are 1.4 cm and 2.2 cm, respectively.

PXD module

PXD Sensor / Module

- Sensor:
  - Self-supporting 75 um thin DEPFET active area.
  - Pixel size: 50x(55-85) um^2.
  - 250 x 768 pixels per sensor.
  - 40 sensors in total.
- Module:
  - DEPFET sensor with ASICs.
  - 6 switchers: row control, 4 rows per channel.
  - 4 DCD: 256 channel 8-bit ADC.
  - 4 DHP: data processing, trigger and timing.
  - 40 modules in total.
- Ladder:
  - Two modules glued to one ladder.
  - 20 ladders in total.
- Design: 1% occupancy (layer 1), 3% occupancy limit (DHP, DAQ, tracking).
- Cooling:
  - 2-phase CO_2 cooling for ASICs at the end of stave.
  - N_2 gas for sensor and switchers.
- Radiation hard sensor and ASICs up to expected lifetime, measured up to 266 kGy during irradiation campaign.

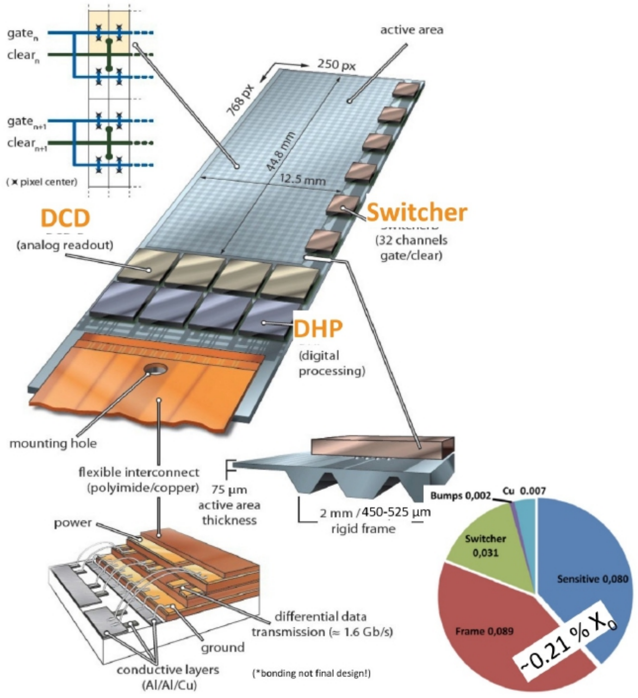

5

PXD Performance: efficiency

- Defined by hits found close to track intercepting points in modules.
- Influenced by tracking quality and alignment.
- Take only tracks with good tracking and $p_T > 1$ GeV/c.
- Bad switcher channels (4 rows each) degrade overall hit efficiency by ~3% (good regions ~ 98% hit efficiency).
- Noisy switcher from May 10th beam loss.
- Module 1032 was broken.
    - Covered by layer 2 module.

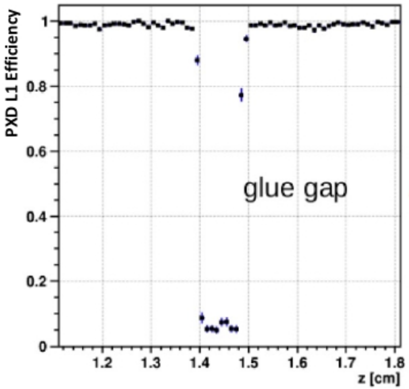

Glue gaps

Half shell gap

Noisy switcher from May 10th beam loss incident

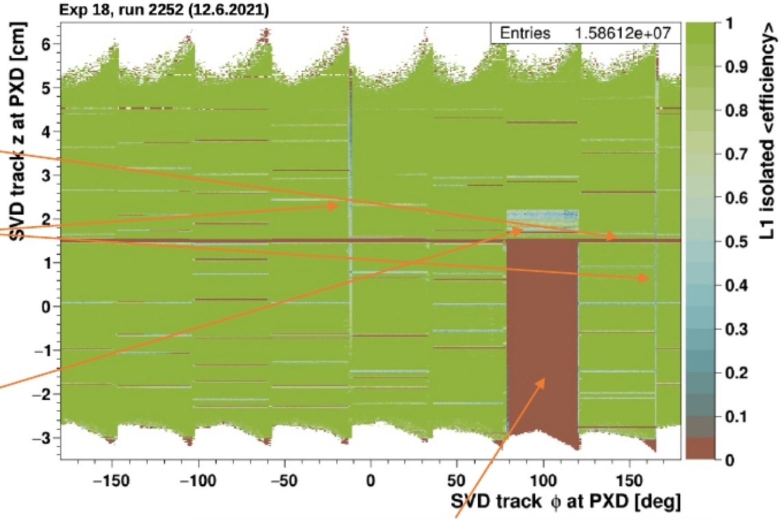

9

Broken module

Principle of fabrication

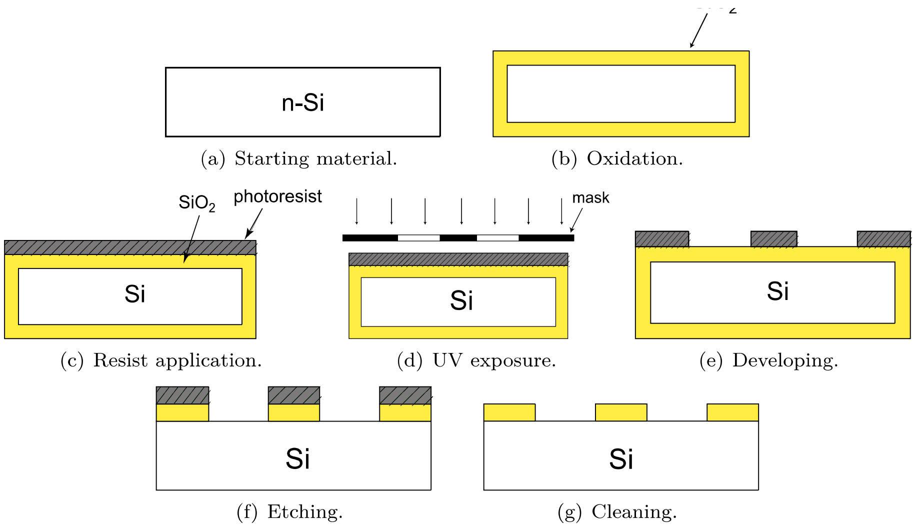

Fig. 8.42 Process steps of photolithography.

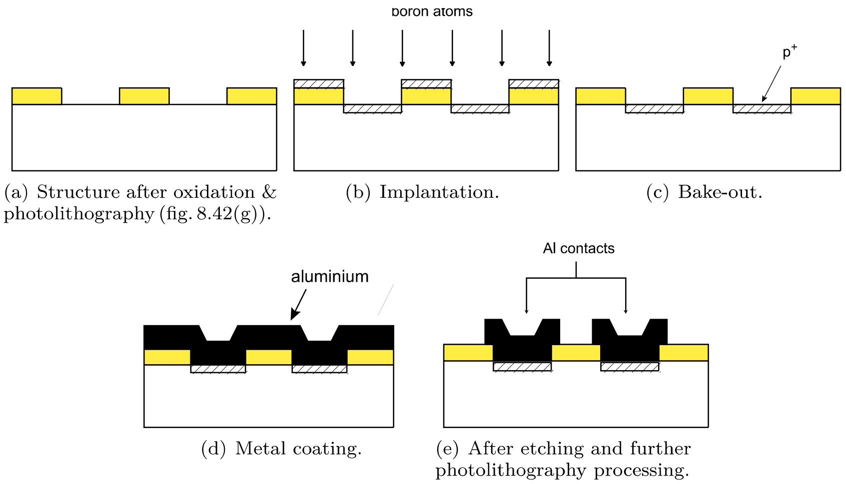

Fig. 8.43 Processing steps in semiconductor structuring (here: p electrodes on n-substrate wafer).

SVD in a nutshell

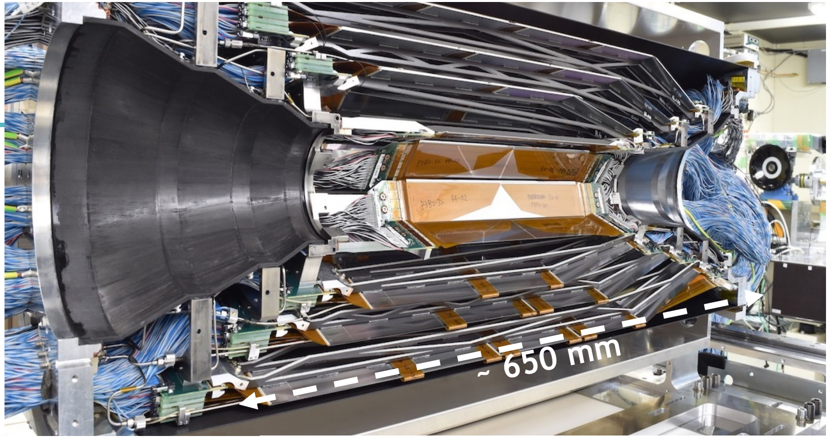

- 4 layers of *Ladders* mounted on end rings supported by carbon fiber structures, covering polar angle θ region from 17° to 150°
    - Barrel shape in L3
    - Lantern shape in L456 (slanted FW sensors) to reduce material
- Signals from each sensors connected with flex circuits to front-end ASICs mounted on the ladder
    - chips outside active area for L3, *chip-on-sensor* for L456 long ladders
- Evaporative CO_2 cooling (-20°C) with thin stainless steel pipes
- Total material budget 0.7% per layer - Total Silicon area 1.2 m^2

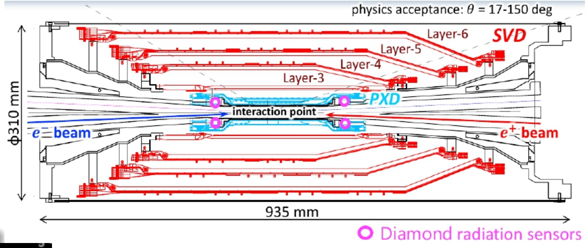

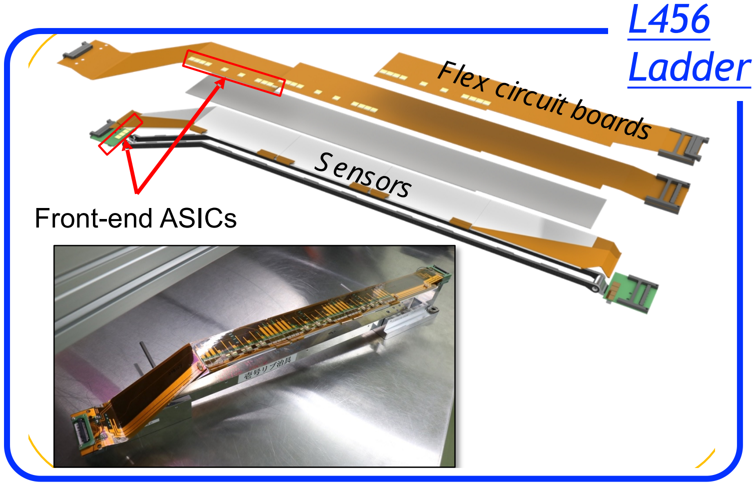

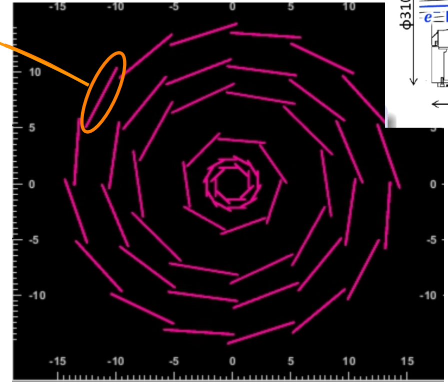

Layer	ladders	sensors	Radius (mm)
L3	7	2	39
L4	10	3	80
L5	12	4	104
L6	16	5	135

SVD sensors and ASIC

Double Sided Strip DSSD

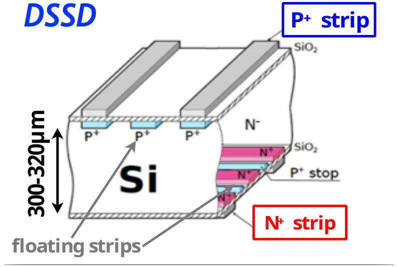

AC coupled strips
Depletion Voltage 20-60V
Operation Voltage 100 V

3 shapes of DSSD used in ladders

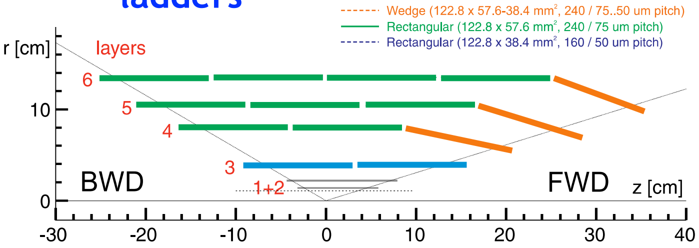

172 sensors

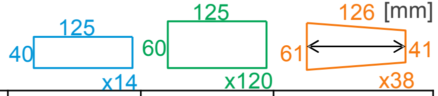

	Small	Large	Trapezoidal
# of p-strips*	768	768	768
p-strip pitch*	50 μm	75 μm	50-75 μm
# of n-strips*	768	512	512
n-strip pitch*	160 μm	240 μm	240 μm
thickness	320 μm	320 μm	300 μm
manufacturer	HPK		Micron

*readout strips – one floating strip on both sides

APV25 chips in

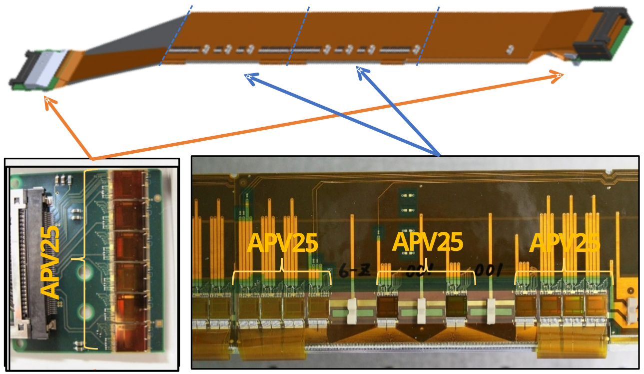

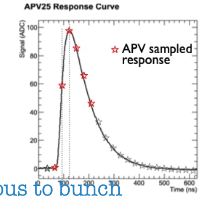

- Fast: 50 ns shaping time
- Rad hard: >100 Mrad
- 128 channels per chip, analog pipeline
- Operated in multi-peak mode @ 32 MHz
  - Collisions every 4 ns & clock not synchronous to bunch crossing as in CMS
  - 6 samples recorded, 3/6 samples in future to reduce data size
- Power consumption 0.4W/chip → 700 W in SVD
- Chip-on-sensor (ORIGAMI) concept:
  - Shorter strip → smaller capacitance & low noise
  - APV chips thinned to 100 um to reduce material
  - Thin stainless steel pipes (two phase CO2 cooling @-20°C) only on one side of the sensor!

SVD Resolution

- Cluster position resolution measured using $e^+e^- \to \mu^+\mu^-$.
- The resolution is estimated from the residual between the cluster position and the track position, after subtracting the effect of the track extrapolation error.
  - Sensor Under Test not included in track fitting to avoid bias.

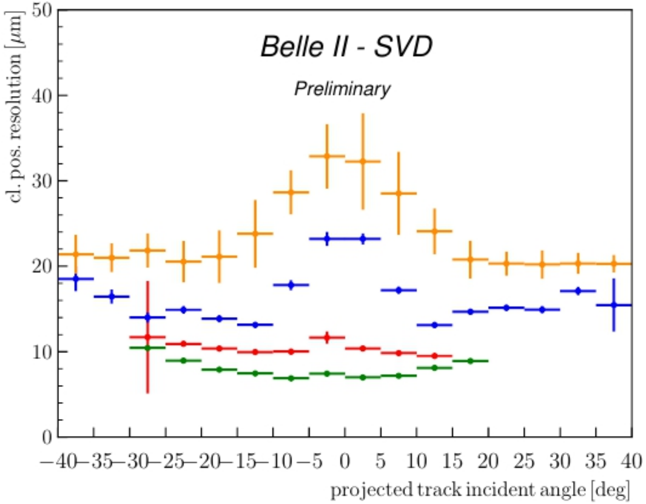

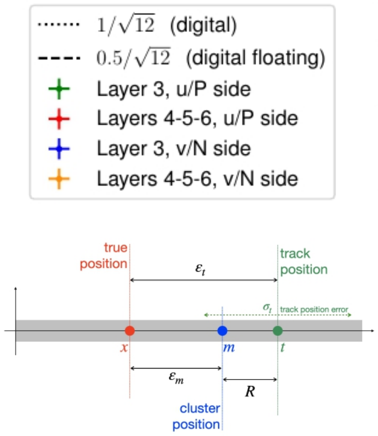

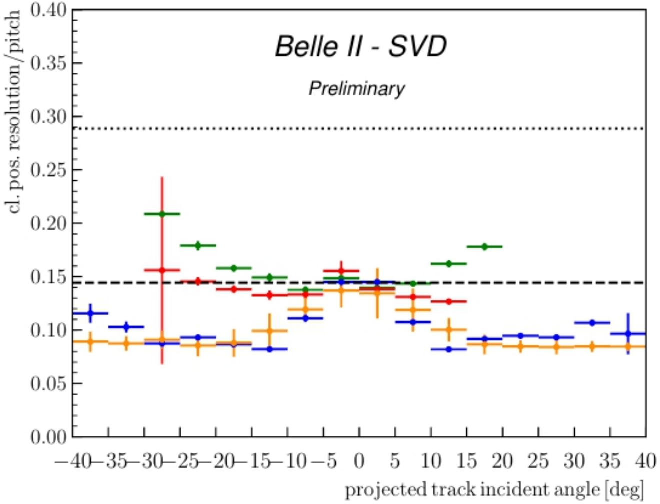

SVD Perfromance: Signal to Noise

- Signal charge normalised for the track path length in silicon similar in all sensors and matches expectations
  - u/P side: charge in agreement with expectation from MIP taking into account a 15% uncertainty in APV25 gain calibration
  - v/N side: 10%-30% signal loss due to large pitch and presence of floating strip

Normalized for path length (320 μm)

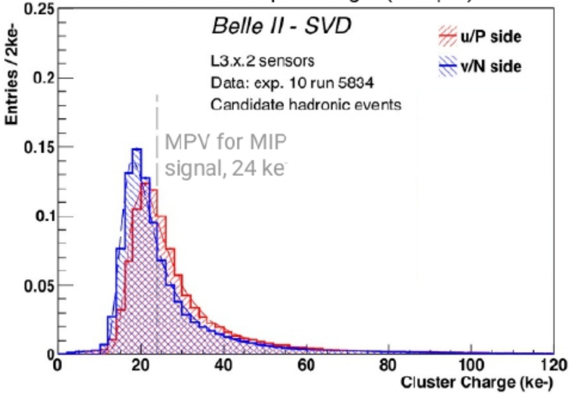

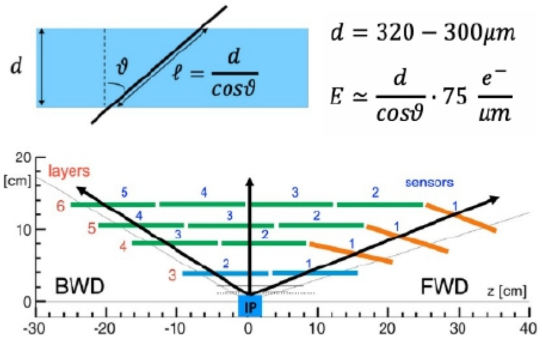

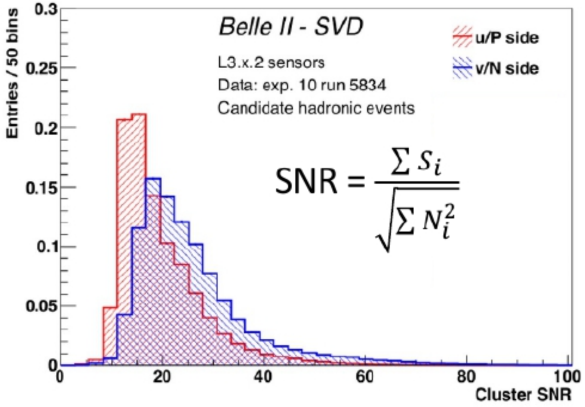

Vertex detector perfomance

- Vertex resolution with PXD is close to MC expectations.
  - d_0 resolution of 14.1 um (data), 12.5 um (MC).
- D lifetime measurement:
  - 4th Belle II physics paper, submitted to PRL, arXiv: 2108.03126.
  - Belle II proper time resolution ~2x better than Belle.
  - Precision better than all previous measurements and comparable with world average.
  - Vertex detectors played key role in this measurement.

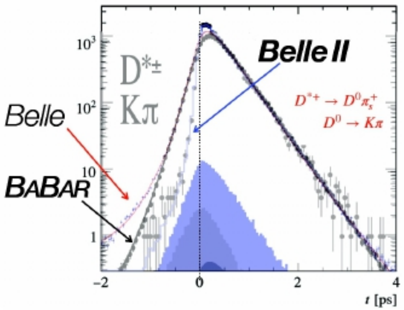

$\tau(D^0) = 410.5 \pm 1.1$ (stat) ± 0.8 (syst) fs
$\tau(D^+) = 1030.4 \pm 4.7$ (stat) ± 3.1 (syst) fs

World Average
(410.1 ± 1.5) fs
(1040 ± 7) fs

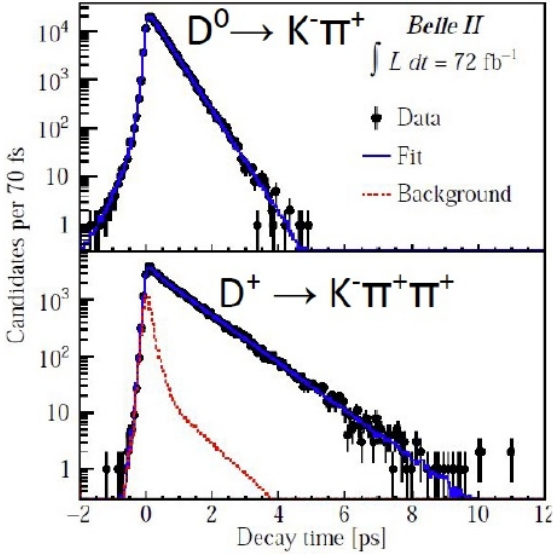

Sources and references

- Main reference:
  - H. Kolanoski, N. Wermes – Particle detectors – Oxford University Press (2020)
- Books:
  - S.N.Ahmed – Physics and Engineering of Radiation Detectors, Elsevier 2015
  - W.R. Leo – Techniques for Nuclear and Particle Physics Experiments, Springer 1994
  - G.F. Knoll – Radiation detection and measurement, Wiley 1989
  - K.Kleinknecht – Detectors for Particle Radiation, Cambridge, 1998
  - C.Grupen – Particle Detectors, Cambridge, 2009
  - T.Ferbel, ed. – Experimental Techniques in High Energy Physics, World Scientific, 1991
  - H.Spieler - Semiconductor Detector Systems, Oxford UP (2005)
- Lessons
  - E. Garutti Slides at DESY
  - H.-C. Schultz-Coulon & J. Stachel Slides at Heidelberg
  - H. Spieler – website on semiconductor detectors and electronics
  - Various speakers - EDIT school 2011, Silicon strip and pixels technologies, Part1 & Part2
  - T.Bergauer - Silicon detectors in high energy physics, slides at HEPHY
- Particle Data Group - The Review of Particle Physics
  - https://pdg.lbl.gov/

EXTRAS

Electrode patterning

Tipical strip pitch: 100um
n- = lightly doped n-type
n+, p+ = heavily doped

- Many possible geometries
- Guard rings often used to reduce the electric field on the edge of the sensor

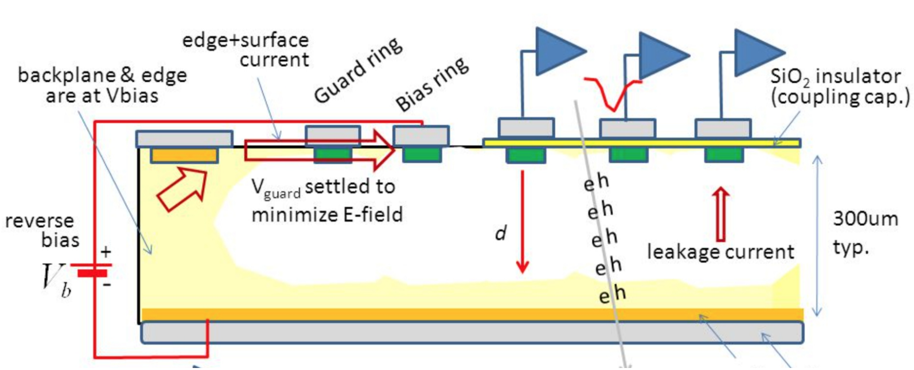

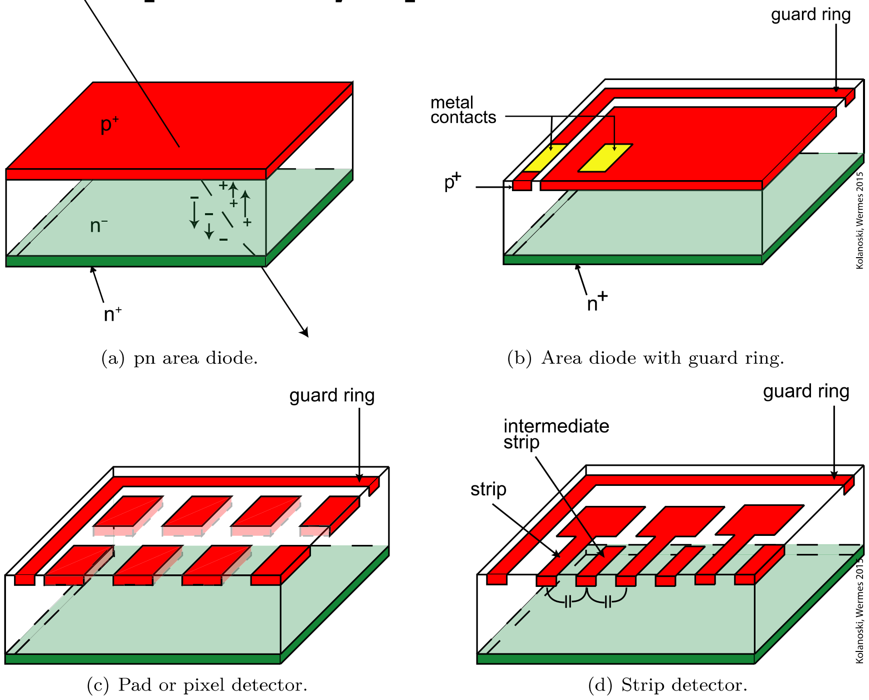

Fig. 8.35 Design concepts of single-sidedly processed pn detectors. The labels n^+ and n^-, respectively, denote strong/weak n doping, correspondingly for p doping (see also footnote on 285). Author: P. Fischer.